

# FREE-FIELD RESOLUTIONS OF THE UNITARY $N=2$ SUPER-VIRASORO REPRESENTATIONS

B. L. FEIGIN AND A. M. SEMIKHATOV

ABSTRACT. We construct free-field resolutions of unitary representations of the  $N=2$  superconformal algebra. The irreducible representations are singled out from free-field spaces as the cohomology of fermionic screening operators. We construct and evaluate the cohomology of the resolution associated with one fermionic screening (which is related to the representation theory picture of “gravitational descendants”), and a *butterfly* resolution associated with two fermionic screenings.

## CONTENTS

1. Introduction	1
2. Generalities	3
2.1. The $N=2$ algebra and the spectral flow	3
2.2. Unitary representations of the $N=2$ algebra	4
3. The ghost realisation	5
3.1. Modding, etc., of the ghost systems	5
3.2. The structure of the ghost realisation: “gravitational descendants” and the resolution	6
3.3. Mapping to the Wakimoto bosonisation	11
3.4. End of the proof of Theorem 3.1	13
4. The “symmetric” realisation	15
4.1. Generalities	15
4.2. The butterfly resolution	17
4.3. Jamming the butterfly into the two-sided resolution	21
5. Conclusions	23
Appendix A. $N=2$ Verma modules	24
References	26

## 1. INTRODUCTION

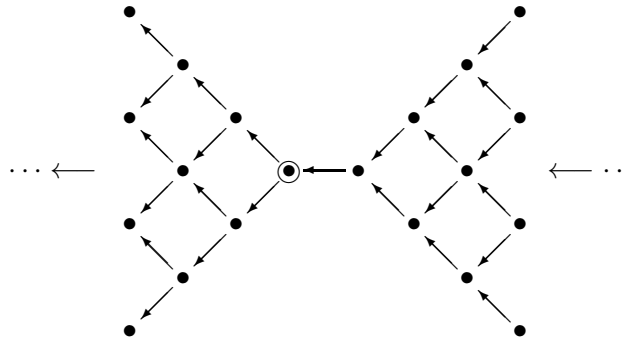
As is well known, free-field constructions (“bosonisations”) of infinite-dimensional algebras alter the embedding structure of Verma-like modules [1]; resolutions of irreducible representations are also changed, the classical example being that of the BGG resolution [2] of irreducible Virasoro representations replaced by the Felder resolution [3]. The resolutions associated with bosonisations are related to the screening operators existing in free-field representation spaces (in fact, to the corresponding quantum-group structure) [3, 4, 5, 6].

Several free-field constructions of the  $N=2$  superconformal extension of the Virasoro algebra are known. One of these [7, 8] has been used in the analysis of the Landau–Ginzburg (LG) models [8, 9, 10]. There also exist a bosonisation [11, 12, 13] with two fermionic screening operators, and the  $N=2$  construction [14, 15] realised in the bosonic string (although the latter is not necessarily a *free*-field realisation). Despite the wide use of free-field constructions, however, the corresponding resolutions of

irreducible  $N=2$  representations have not been written out (resolutions of irreducible  $N=2$  representations in terms of *Verma* modules were constructed in [16]). In this paper, we fill this gap for unitary  $N=2$  representations [17] by constructing resolutions associated with *fermionic* screenings.

The first resolution that we construct is in the space of a bosonic ( $bc$ ) and a fermionic ( $\beta\gamma$ ) ghost systems (which is a particular case of the realisation used in the LG context [8, 9, 10], the  $N=2$  supersymmetry in the  $bc\beta\gamma$  system being known since [18]). The resolution is of a “linear” two-sided structure, and in this respect is similar to the  $\widehat{sl}(2)$  resolution [4, 5] associated with the Wakimoto bosonisation. However, it is *not* the image under the  $\widehat{sl}(2) \leftrightarrow N=2$  correspondence [19, 20] of the known  $\widehat{sl}(2)$  resolution; instead, its  $\widehat{sl}(2)$  counterpart is constructed of *twisted* (spectral-flow transformed) modules.<sup>1</sup> A half of the  $N=2$  resolution consists of the modules generated from the gravitational descendants [22, 23, 24] of the highest-weight vector in the cohomology.

Another free-field realisation [11, 12, 13] that we consider here involves two screening operators, which are both fermions. These give rise to the *butterfly resolution*



(1.1)

whose two-winged shape seems to be an entirely new structure. In both cases, however, the cohomology is given by the unitary  $N=2$  representations (Theorems 3.1 and 4.2). Recall that the unitary  $N=2$  representations are characterised by the relation

$$(1.2) \quad \partial^{p-2}\mathcal{G}(z) \dots \partial\mathcal{G}(z) \mathcal{G}(z) = 0,$$

where  $\mathcal{G}(z)$  is one of the two fermionic fields entering the  $N=2$  superconformal algebra. This gives an alternative way to show that the cohomology is a sum of unitary representations: it suffices to check the action of the  $N=2$  algebra and to verify that (1.2) is satisfied (in the  $bc\beta\gamma$  realisation, for example, the latter condition holds because the  $\gamma(z)$  field satisfies  $\gamma^{p-1} = 0$  in the cohomology).

The general features that are important in the analysis of  $N=2$  representations (and which are absent in the Virasoro and  $N=1$  superconformal algebras) are the spectral flow transform [25] and the appearance of *twisted*—spectral-flow-transformed—(sub)modules, even if one starts with an “untwisted” module [21]. The spectral flow maps between different unitary  $N=2$  representations, the length of the orbit being  $p$  (or  $p/2$  in a certain special case of even  $p$ ) [19, 16], where  $p = (2), 3, 4, \dots$  parametrises the central charge. Thus, all of the unitary representations can be obtained by applying the spectral flow to only  $[p/2]$  representatives of the spectral flow orbits, and similarly for the resolutions.

<sup>1</sup>We systematically refer to the modules transformed by the spectral flow as *twisted* modules, see [19, 21, 16].

As with all the “invariant” structures pertaining to  $N=2$  representations, the resolutions we construct have their  $\widehat{sl}(2)$  counterparts. We will comment on how the two resolutions are mapped into the Wakimoto bosonisation [26, 27, 28] of  $\widehat{sl}(2)$ . From a more general perspective, different free-field realisations are particular cases of the three-boson realisation of the  $N=2$  (or  $\widehat{sl}(2)$ ) algebra. We do not attempt here to analyse the generic three-boson realisation resolutions, which should include (i) the case of a bosonic and a fermionic screening that make up the nilpotent subalgebra of  $sl(2|1)_q$ , and another bosonic screening commuting with the first two; as regards the “ $sl(2|1)_q$ -pair,” we hope to consider it in the future, while taking a bosonic and a fermionic screening that commute with each other leads eventually to the Felder-type resolution, since the fermionic screening singles out a  $\beta\gamma$  system, after which the bosonic screening acts as in [4, 5]; (ii) the case of two fermionic screenings and a non-vertex-operator bosonic screening. This also has not been worked out in general, but what we consider in Sec. 4 is an important particular case—that of integrable representations—where the fermionic screenings commute (and, thus, make it possible to consider the resolution with one fermionic screening as in Sec. 3).

In Sec. 2, we recall some basic facts about the  $N=2$  superconformal algebra and its unitary representations. In Sec 3, we consider the  $bc\beta\gamma$  realisation of the  $N=2$  algebra. We evaluate the BRST cohomology of the fermionic screening and show how the corresponding resolution gives rise to gravitational descendant fields. In Sec. 4, we consider the bosonisation in terms of a complex scalar and a fermionic ghost system and construct the butterfly resolution, whose cohomology is also given by the unitary  $N=2$  representations. We also discuss the relation between the two resolutions.

## 2. GENERALITIES

**2.1. The  $N=2$  algebra and the spectral flow.** The  $N=2$  superconformal algebra is taken in the basis where the nonvanishing commutation relations read as

$$\begin{aligned}
 (\mathcal{L}_m, \mathcal{L}_n) &= (m-n)\mathcal{L}_{m+n}, & (\mathcal{H}_m, \mathcal{H}_n) &= \frac{c}{3}m\delta_{m+n,0}, \\
 (\mathcal{L}_m, \mathcal{G}_n) &= (m-n)\mathcal{G}_{m+n}, & (\mathcal{H}_m, \mathcal{G}_n) &= \mathcal{G}_{m+n}, \\
 (\mathcal{L}_m, \mathcal{Q}_n) &= -n\mathcal{Q}_{m+n}, & (\mathcal{H}_m, \mathcal{Q}_n) &= -\mathcal{Q}_{m+n}, \\
 (\mathcal{L}_m, \mathcal{H}_n) &= -n\mathcal{H}_{m+n} + \frac{c}{6}(m^2+m)\delta_{m+n,0}, \\
 \{\mathcal{G}_m, \mathcal{Q}_n\} &= \mathcal{L}_{m+n} - n\mathcal{H}_{m+n} + \frac{c}{6}(m^2+m)\delta_{m+n,0},
 \end{aligned}
 \tag{2.1}$$

with  $m, n \in \mathbb{Z}$ . Here,  $\mathcal{L}_n$  and  $\mathcal{H}_n$  are bosonic, and  $\mathcal{G}_n$  and  $\mathcal{Q}_n$ , fermionic elements. In what follows, we do not distinguish between the central element  $C$  and its eigenvalue  $c$ , which we assume to be  $c \neq 3$  and parametrise as  $c = 3(1 - \frac{2}{t})$  with  $t \in \mathbb{C} \setminus \{0\}$ . In the unitary case, we write  $t = p = 2, 3, \dots$  (where  $p=2$  leads to the trivial representation). To describe the same algebra in terms of *currents* and operator products, we define  $\mathcal{Q}(z) = \sum_{n \in \mathbb{Z}} \mathcal{Q}_n z^{-n-1}$ ,  $\mathcal{G}(z) = \sum_{n \in \mathbb{Z}} \mathcal{G}_n z^{-n-2}$ ,  $\mathcal{T}(z) = \sum_{n \in \mathbb{Z}} \mathcal{L}_n z^{-n-2}$ , and  $\mathcal{H}(z) = \sum_{n \in \mathbb{Z}} \mathcal{H}_n z^{-n-1}$ .

In the basis chosen in (2.1), the spectral flow [25] acts as

$$(2.2) \quad \begin{aligned} \bar{U}_\theta : \quad \mathcal{L}_n &\mapsto \mathcal{L}_n + \theta \mathcal{H}_n + \frac{\varepsilon}{6}(\theta^2 + \theta)\delta_{n,0}, & \mathcal{H}_n &\mapsto \mathcal{H}_n + \frac{\varepsilon}{3}\theta\delta_{n,0}, \\ \mathcal{Q}_n &\mapsto \mathcal{Q}_{n-\theta}, & \mathcal{G}_n &\mapsto \mathcal{G}_{n+\theta}. \end{aligned}$$

For  $\theta \in \mathbb{Z}$ , these transformations are automorphisms of the algebra. Allowing  $\theta$  to be half-integral in (2.2), we obtain the isomorphism between the Ramond and Neveu–Schwarz sectors. We refer to the modules subjected to the action of the spectral flow as *twisted* modules; the algebra acts on a twisted module according to the standard prescription that “a given generator acts as the spectral-flow transformed generator acts on the original module.”

**2.2. Unitary representations of the  $N=2$  algebra.** We now briefly review, following [16], several facts about the unitary  $N=2$  representations. These are the irreducible quotients of the twisted topological<sup>2</sup> Verma modules (see the Appendix or [21, 29] for more details)  $\mathfrak{V}_{\mathfrak{h}^+(r,1,p),p;\theta}$ , where the variable parametrising the central charge is  $t = p \in \mathbb{N} + 1$ ,<sup>3</sup>  $\mathfrak{h}^+$  is defined in (A.4),  $r$  is an integer such that  $1 \leq r \leq p-1$ , and  $\theta$  is the twist (see Definition A.1). Although the Verma module can be taken with any integral twist  $\theta$ , the unitary representations are periodic with period  $p$  (i.e., acting with the spectral flow transform with  $\theta = p$  gives an isomorphic representation):

$$(2.3) \quad \mathfrak{K}_{r,p;\theta+p} \approx \mathfrak{K}_{r,p;\theta}.$$

For the unitary representations, the twist  $\theta$  can therefore be considered mod  $p$ ; thus, the unitary representations are labelled by

$$(2.4) \quad \mathfrak{K}_{r,p;\theta}, \quad 1 \leq r \leq p-1, \quad \theta \in \mathbb{Z}_p.$$

Among these, *there are only  $p(p-1)/2$  non-isomorphic unitary representations*, since there exist the  $N=2$  isomorphisms

$$(2.5) \quad \mathfrak{K}_{r,p;\theta+r} \approx \mathfrak{K}_{p-r,p;\theta}, \quad 1 \leq r \leq p-1, \quad \theta \in \mathbb{Z}_p.$$

Thus, in order to count each unitary representation once, we can, for example, take  $1 \leq r \leq [p/2]$  with the full range of  $\theta$ ,  $0 \leq \theta \leq p-1$ , or allow  $1 \leq r \leq p-1$  with  $0 \leq \theta \leq r-1$ . There is a special periodicity property applying to the representations  $\mathfrak{K}_{r,2r;\theta}$ , for which the period is half that of Eq. (2.3):  $\mathfrak{K}_{r,2r;\theta+r} \approx \mathfrak{K}_{r,2r;\theta}$ .

As noted in the Introduction, the structure of all the unitary representations is described once this is done for a representative of each spectral flow orbit. In the next section, for example, we concentrate on the representations  $\mathfrak{K}_{r,p;r-1}$ , which in terms of the Verma modules are the quotients (see (A.9))

$$(2.6) \quad \mathfrak{K}_{r,p;r-1} = \mathfrak{V}_{\frac{1-r}{p},p;r-1} / \left( \mathfrak{V}_{\frac{r+1}{p}-2,p;p-1} + \mathfrak{V}_{\frac{r+1}{p},p;-1} \right).$$

The untwisted representations will also be denoted by  $\mathfrak{K}_{r,p} \equiv \mathfrak{K}_{r,p;0}$ .

<sup>2</sup> *Chiral* modules in a different nomenclature [36].

<sup>3</sup>  $\mathbb{N} = \{1, 2, \dots\}$  and, for the future use,  $\mathbb{N}_0 = \{0, 1, 2, \dots\}$ .

## 3. THE GHOST REALISATION

The free-field realisation of the  $N=2$  algebra that we consider here has a known relation to the  $A_{p-1}$  LG models. Given a sum  $W(\gamma_1, \dots, \gamma_n)$  of the  $A$ -series LG potentials, one constructs the Koszul differential associated with the LG “equations of motion”  $\partial W / \partial \gamma_i = 0$  [7, 8, 9]; for an individual  $A_{p-1}$  model, this differential is

$$(3.1) \quad \mathbb{Q}_0 = \frac{1}{2\pi i} \oint c \gamma^{p-1},$$

which, according to the standard BRST ideology, imposes the constraint

$$(3.2) \quad \gamma(z)^{p-1} \approx 0.$$

The  $c$  and  $\gamma$  fields involved in (3.1) are viewed as the respective halves of a  $bc$  (fermionic) and a  $\beta\gamma$  (bosonic) first-order systems with the operator products

$$(3.3) \quad b(z)c(w) = \frac{1}{z-w}, \quad \beta(z)\gamma(w) = \frac{-1}{z-w}.$$

Then [7, 8]  $\mathbb{Q}_0$  commutes with (is the screening of) the  $N=2$  algebra realised in terms of the *currents*  $\mathcal{Q}(z)$  etc. as

$$(3.4) \quad \begin{aligned} \mathcal{Q} &= -\beta c, \\ \mathcal{G} &= -\frac{1}{p}\gamma\partial b - \left(\frac{1}{p} - 1\right)\partial\gamma b, \\ \mathcal{H} &= -\frac{1}{p}\beta\gamma + \left(1 - \frac{1}{p}\right)bc, \\ \mathcal{T} &= \frac{1}{p}\partial b c - \left(1 - \frac{1}{p}\right)b\partial c + \frac{1}{p}\partial\beta\gamma - \left(1 - \frac{1}{p}\right)\beta\partial\gamma. \end{aligned}$$

This algebra helps organise the cohomology of  $\mathbb{Q}_0$ , which, as could be expected [8, 9], is given by a sum of unitary  $N=2$  representations (Eq. (3.15)). To this end, we construct the resolution, which will in turn require analysing the representations of (3.4) in some detail. We assume, as before,  $p \in \mathbb{N} + 1$ . We now digress to fix the conventions regarding ghost systems.

**3.1. Modding, etc., of the ghost systems.** We will consider the  $bc$  and  $\beta\gamma$  fields with a fractional modding, i.e., with “twisted boundary conditions.” We assume the point of view that twisted boundary conditions on fermions give rise to a fractional fermion number of the vacuum. For first-order fields of a (half-)integer spin  $\lambda$ , it is convenient to introduce the Fourier modes as  $b(z) = \sum b_n z^{-n-\lambda}$  and  $c(z) = \sum c_n z^{-n-1+\lambda}$ , and impose the annihilation conditions on the  $n$ th-picture vacuum as

$$(3.5) \quad b_{m+1-\lambda-n} |n\rangle_{bc} = 0, \quad c_{m+\lambda+n} |n\rangle_{bc} = 0, \quad m = 0, 1, 2, \dots$$

Then it follows that  $(bc)_0 |n\rangle_{bc} = n |n\rangle_{bc}$ . We continue these relations to the case of rational  $\lambda$  and the picture number  $n$ .

In what follows, the  $bc$  and  $\beta\gamma$  picture numbers  $n$  and  $\nu$  will be fractions such that

$$(3.6) \quad p\nu \in \mathbb{Z}, \quad \nu - n \in \mathbb{Z}.$$

The ghost systems in (3.4) have conformal spin

$$(3.7) \quad \lambda = 1 - \frac{1}{p}.$$

Thus, the modding of the ghost fields is taken as

$$(3.8) \quad \begin{aligned} b_m, \quad m \in \frac{1}{p} - n + \mathbb{Z}, \quad c_m, \quad m \in -\frac{1}{p} + n + \mathbb{Z}, \\ \beta_m, \quad m \in \frac{1}{p} - \nu + \mathbb{Z}, \quad \gamma_m, \quad m \in -\frac{1}{p} + \nu + \mathbb{Z}. \end{aligned}$$

We define the  $bc$  module  $\Lambda_\lambda(n)$  with the cyclic vector  $|n\rangle_{bc}$  and the  $\beta\gamma$  module  $\Xi_\lambda(\nu)$  with the cyclic vector  $|\nu\rangle_{\beta\gamma}$  subjected to the annihilation conditions

$$(3.9) \quad b_{\geq 1-\lambda-n} |n\rangle_{bc} = 0, \quad c_{\geq \lambda+n} |n\rangle_{bc} = 0,$$

$$(3.10) \quad \beta_{\geq 1-\lambda-\nu} |\nu\rangle_{\beta\gamma} = 0, \quad \gamma_{\geq \lambda+\nu} |\nu\rangle_{\beta\gamma} = 0,$$

where  $n$  and  $\nu$  are as in (3.6) and where we use the convention that  $b_{\geq 1-\lambda-n}$  means  $(b_{m+1-\lambda-n})_{m \in \mathbb{N}_0}$  and  $c_{\geq \lambda+n}$  means  $(c_{m+\lambda+n})_{m \in \mathbb{N}_0}$  (here,  $\Lambda_\lambda(n)$  and  $\Lambda_\lambda(n')$  are of course isomorphic whenever  $n - n' \in \mathbb{Z}$ ). Then,

$$(3.11) \quad (bc)_0 |n\rangle_{bc} = n |n\rangle_{bc},$$

$$(3.12) \quad (\beta\gamma)_0 |\nu\rangle_{\beta\gamma} = -\nu |\nu\rangle_{\beta\gamma}.$$

It follows, in particular, that the modes of the current  $\mathbb{Q}(z) = c(z) \gamma(z)^{p-1}$  read as

$$\mathbb{Q}_j = \sum_{m_1, \dots, m_{p-1} \in \mathbb{Z} - \frac{1}{p}} c_{j-m_1-\dots-m_{p-1}} \gamma_{m_1} \cdots \gamma_{m_{p-1}}$$

with  $j \in \mathbb{Z}$ , which is consistent because  $-m_1 - \dots - m_{p-1} \in (p-1)\frac{1}{p} - (p-1)\nu + \mathbb{Z} = -\frac{1}{p} + \nu + \mathbb{Z} = -\frac{1}{p} + n + \mathbb{Z}$  in view of (3.6).

For the  $N = 2$  representation generated from the vector  $|n\rangle_{bc} \otimes |\nu\rangle_{\beta\gamma} \in \Lambda_\lambda(n) \otimes \Xi_\lambda(\nu)$ , the  $N = 2$  spectral flow transform  $\mathcal{U}_\vartheta$  is realised by changing the  $bc$  and  $\beta\gamma$  pictures as

$$(3.13) \quad \Lambda_\lambda(n) \rightarrow \Lambda_\lambda(n - \vartheta\lambda), \quad \Xi_\lambda(\nu) \rightarrow \Xi_\lambda(\nu + \vartheta(1 - \lambda)).$$

For  $\vartheta \notin p\mathbb{Z}$ , pictures are changed by non-integer numbers, thereby leading to an inequivalent representation even in the  $bc$  sector alone (while the spectral flow with  $\vartheta \in p\mathbb{Z}$ , although changing the  $\beta\gamma$  representation, induces an isomorphism on the cohomology, as we will see). Anyway, this realisation of the  $N = 2$  spectral flow allows us to fix the overall twist in an arbitrary way until the very end, when the spectral flow transform with any desired  $\vartheta$  can be applied to the free-field representations. In what follows, it will be convenient to fix the twist as  $r - 1$ ; we will arrive at the unitary representation  $\mathfrak{K}_{r,p;r-1}$ , Eq. (2.6).

### 3.2. The structure of the ghost realisation: “gravitational descendants” and the resolution.

We now describe a complex of  $N = 2$  representations on the  $bc\beta\gamma$  space  $\Lambda_\lambda(n) \otimes \Xi_\lambda(\nu)$  whose cohomology gives the unitary  $N = 2$  representations. Recall that the  $bc\beta\gamma$  system is an essential ingredient of the conformal field theory description of topological gravity [30, 31], where this system gives rise to the gravitational descendants [22, 23, 24] of primary fields. The representation-theoretic picture of the gravitational descendants will also be seen from the complex (Remark 3.2).

*Notation for the modules.* A Verma module  $\mathfrak{U}_{h,\ell,p;\theta}$  (see (A.10)–(A.12)) is uniquely characterised by  $(h, \ell, p; \theta)$ , i.e., by the highest-weight conditions (including the Cartan eigenvalues) satisfied by the

highest-weight vector. In the free-field realisation, on the contrary, a given module is not characterised by the highest-weight conditions satisfied by the vector(s) from which the module is generated. However, indicating the values of  $h$ ,  $\ell$ , and  $\theta$  is still very useful in the analysis of mappings between modules. We will thus use the notation  $\widehat{\mathfrak{U}}_{h,\ell,p;\theta}(M, N)$  for the module generated from  $|M\rangle_{bc} \otimes \gamma_{\lambda+\nu-1}^N |\nu\rangle_{\beta\gamma}$  for  $N \geq 0$ , or from  $|M\rangle_{bc} \otimes \beta_{-\lambda-\nu}^{-N} |\nu\rangle_{\beta\gamma}$  for  $N < 0$ , once this vector satisfies the same highest-weight conditions as the twisted massive highest-weight vector  $|h, \ell, p; \theta\rangle$ ; we also write  $\widehat{\mathfrak{W}}_{h,p;\theta}(M, N)$  for the module generated from  $|M\rangle_{bc} \otimes \gamma_{\lambda+\nu-1}^N |\nu\rangle_{\beta\gamma}$ ,  $N \geq 0$  (or  $|M\rangle_{bc} \otimes \beta_{-\lambda-\nu}^{-N} |\nu\rangle_{\beta\gamma}$ ,  $N < 0$ ) when this vector satisfies the same highest-weight conditions as the twisted topological highest-weight vector  $|h, p; \theta\rangle_{\text{top}}$ . Moreover, we will in some cases omit the arguments  $(M, N)$  altogether, simply indicating the ghost realisation of the highest-weight vector of the module the first time the module appears.

**Theorem 3.1.** *Let  $\mathfrak{G}_{n,\nu,p} = \Lambda_\lambda(n) \otimes \Xi_\lambda(\nu)$ ,  $\lambda = 1 - \frac{1}{p}$ , be the ghost representation space defined in accordance with (3.9)–(3.12), where  $n, \nu \in \frac{1}{p}\mathbb{Z}$ ,  $\nu - n \in \mathbb{Z}$ , and*

$$1 + (\nu + 1)(1 - p) \leq n \leq \nu(1 - p).$$

*Then there is a complex of  $N=2$  representations on  $\mathfrak{G}_{n,\nu,p}$*

$$(3.14) \quad \dots \xrightarrow{\mathbb{Q}_0} \widehat{\mathfrak{U}}_{\frac{r+1}{p}-m-1,0,p;p-1+\nu p} \xrightarrow{\mathbb{Q}_0} \dots \xrightarrow{\mathbb{Q}_0} \widehat{\mathfrak{U}}_{\frac{r+1}{p}-2,0,p;p-1+\nu p} \xrightarrow{\mathbb{Q}_0} \widehat{\mathfrak{U}}_{\frac{r+1}{p},0,p;\nu p-1} \xrightarrow{\mathbb{Q}_0} \dots$$

$$\xrightarrow{\mathbb{Q}_0} \widehat{\mathfrak{U}}_{\frac{r+1}{p}+1,0,p;\nu p-1} \xrightarrow{\mathbb{Q}_0} \dots \xrightarrow{\mathbb{Q}_0} \widehat{\mathfrak{U}}_{\frac{r+1}{p}+m,0,p;\nu p-1} \xrightarrow{\mathbb{Q}_0} \dots$$

where  $r = 1 + \nu(1 - p) - n$ , the modules  $\widehat{\mathfrak{U}}_{\frac{r+1}{p}+m,0,p;\nu p-1}$  with  $m \geq 0$  are generated by the  $N=2$  generators (3.4) from the states  $|1 + \nu(1 - p)\rangle_{bc} \otimes \gamma_{\lambda+\nu-1}^{mp+r} |\nu\rangle_{\beta\gamma} \in \Lambda_\lambda(n) \otimes \Xi_\lambda(\nu)$ , and the modules  $\widehat{\mathfrak{U}}_{\frac{r+1}{p}-m,0,p;p-1+\nu p}$ ,  $m \geq 2$ , from  $|2 - p + \nu(1 - p)\rangle_{bc} \otimes \beta_{-\lambda-\nu}^{mp-r-1} |\nu\rangle_{\beta\gamma}$ . The cohomology of (3.14) is concentrated at the term  $\widehat{\mathfrak{U}}_{\frac{r+1}{p},0,p;\nu p-1}(1 + \nu(1 - p), r)$  and is given by the unitary  $N=2$  representation  $\mathfrak{K}_{r,p;\theta}$  with

$$r = 1 + \nu(1 - p) - n, \quad \theta = \nu - n.$$

Since  $\Lambda_\lambda(n) \approx \Lambda_\lambda(n')$  whenever  $n - n' \in \mathbb{Z}$ , we obtain

**Corollary.** *The cohomology of  $\mathbb{Q}_0$  on  $\mathfrak{G}_{n,\nu,p}$  is given by the direct sum of unitary  $N=2$  representations*

$$(3.15) \quad \bigoplus_{r=1}^{p-1} \mathfrak{K}_{r,p;r-1+\nu p}.$$

The data in the conditions of the Theorem are invariant under the shifts

$$(3.16) \quad n \mapsto n + a(1 - p), \quad \nu \mapsto \nu + a,$$

which change the twist as  $\theta \mapsto \theta + pa$ . For  $a \in \mathbb{Z}$ , this induces the isomorphism (2.3) of the unitary representations. For a *non-integral*  $a \in \frac{1}{p}\mathbb{Z}$ , such a shift leads to another unitary  $N=2$  representation, however the difference amounts to the overall spectral flow transform, which is applied to the ghost spaces in accordance with (3.13). Thus, the theorem is *equivalent* to its  $\nu = 0$ -case, which reads as follows.

**Theorem 3.1** <sup>$\nu=0$</sup> . *Let  $1 \leq r \leq p-1$  and let  $\mathfrak{G}_{1-r,0,p} = \Lambda_\lambda(1-r) \otimes \Xi_\lambda(0) \approx \Lambda_\lambda(0) \otimes \Xi_\lambda(0)$ ,  $\lambda = 1 - \frac{1}{p}$ , be the ghost representation space. Then there is a complex*

$$(3.17) \quad \dots \rightarrow \hat{\mathfrak{U}}_{\frac{r+1}{p}-m,0,p;p-1} \rightarrow \dots \rightarrow \hat{\mathfrak{U}}_{\frac{r+1}{p}-2,0,p;p-1} \rightarrow \\ \rightarrow \hat{\mathfrak{U}}_{\frac{r+1}{p},0,p;-1} \rightarrow \hat{\mathfrak{U}}_{\frac{r+1}{p}+1,0,p;-1} \rightarrow \dots \rightarrow \hat{\mathfrak{U}}_{\frac{r+1}{p}+m,0,p;-1} \rightarrow \dots$$

where the modules  $\hat{\mathfrak{U}}_{\frac{r+1}{p}+m,0,p;-1}$ ,  $m \geq 0$ , are generated by  $N=2$  generators (3.4) from the states  $|1\rangle_{bc} \otimes \gamma_{\lambda-1}^{mp+r}|0\rangle_{\beta\gamma}$ , and the modules  $\hat{\mathfrak{U}}_{\frac{r+1}{p}-m,0,p;p-1}$ ,  $m \geq 2$ , from  $|2-p\rangle_{bc} \otimes \beta_{-\lambda}^{mp-r-1}|0\rangle_{\beta\gamma}$ . The cohomology of (3.17) is concentrated at the term  $\hat{\mathfrak{U}}_{\frac{r+1}{p},0,p;-1}(1,r)$  and is given by the unitary representation  $\mathfrak{K}_{r,p;r-1}$ .

An equivalent form of (3.17) is

$$(3.18) \quad \dots \rightarrow \hat{\mathfrak{V}}_{\frac{1-r}{p}+m-1,p;r-(m-1)p-1}((m-1)p-r+1,0) \rightarrow \dots \rightarrow \hat{\mathfrak{V}}_{\frac{1-r}{p}+1,p;r-p-1}(p-r+1,0) \rightarrow \\ \rightarrow \hat{\mathfrak{U}}_{\frac{r+1}{p},0,p;-1} \rightarrow \hat{\mathfrak{U}}_{\frac{r+1}{p}+1,0,p;-1} \rightarrow \dots \rightarrow \hat{\mathfrak{U}}_{\frac{r+1}{p}+m,0,p;-1} \rightarrow \dots$$

**Remark 3.2.** In (3.17), the modules  $\hat{\mathfrak{U}}_{\frac{r+1}{p}+m,0,p;-1}$ ,  $m \geq 0$ , are generated from the “gravitational descendant” states

$$|1\rangle_{bc} \otimes \gamma_{\lambda-1}^{mp+r}|0\rangle_{\beta\gamma} \equiv \sigma_{(p)}^m(|1\rangle_{bc} \otimes \gamma_{\lambda-1}^r|0\rangle_{\beta\gamma}), \quad \sigma_{(p)} = \gamma_{\lambda-1}^p,$$

which are all  $\mathbb{Q}_0$ -trivial except the original one with  $m=0$ . In the topological gravity, the  $bc\beta\gamma$  states are tensored with primaries from other sectors, which gives the gravitational descendants. As we will see in what follows, the “tic-tac-toe” equations relating the gravitational descendants read as

$$(3.19) \quad \mathcal{Q}_1 |1\rangle_{bc} \otimes \gamma_{\lambda-1}^{(m+1)p+r}|0\rangle_{\beta\gamma} = (mp+r) \mathbb{Q}_0 |1\rangle_{bc} \otimes \gamma_{\lambda-1}^{mp+r}|0\rangle_{\beta\gamma}$$

(these are in fact an essential ingredient in the construction of the resolution). Further,  $\mathcal{Q}_1 |1\rangle_{bc} \otimes \gamma_{\lambda-1}^{mp+r}|0\rangle_{\beta\gamma} = |0\rangle_{bc} \otimes \gamma_{\lambda-1}^{mp+r-1}|0\rangle_{\beta\gamma}$  is a singular vector that satisfies twisted *topological* highest-weight conditions. As in the LG setting, the  $m=0$  state is singled out from these because  $\gamma_{\lambda-1}$  (which in the invariant terms is the top mode of  $\gamma$  that does not annihilate the vacuum) is raised to the power  $0 \leq r-1 \leq k=p-2$ . The effects due to the gravitational dressing have been discussed in different languages (see [32] and references therein, in particular, [15, 33, 22, 23, 24]).

To prove the Theorem, we need to analyse the structure of the ghost realisation.

Consider the  $N=2$  module spanned by generators (3.4) acting on the highest-weight vector  $|n\rangle_{bc} \otimes |\nu\rangle_{\beta\gamma}$ . This state satisfies the same annihilation and eigenvalue equations as the twisted topological highest-weight state  $|(1-\frac{1}{p})\nu + \frac{n}{p}, p; \nu - n\rangle_{\text{top}}$  (see Definition A.1), which we express by writing

$$(3.20) \quad |n\rangle_{bc} \otimes |\nu\rangle_{\beta\gamma} \doteq \left| (1-\frac{1}{p})\nu + \frac{n}{p}, p; \nu - n \right\rangle_{\text{top}}.$$

If, in accordance with the above, the  $\beta\gamma$  system is taken in the zero picture (and hence the  $bc$  picture is integral), we consider the highest-weight vector

$$(3.21) \quad |1-r\rangle_{bc} \otimes |0\rangle_{\beta\gamma} \doteq \left| \frac{1-r}{p}, p; r-1 \right\rangle_{\text{top}}$$



and denote by  $\widehat{\mathfrak{V}}_{\frac{1-r}{p}, p; r-1}(1-r, 0) \subset \Lambda_\lambda(1-r) \otimes \Xi_\lambda(0)$ ,  $\lambda = 1 - \frac{1}{p}$ , the  $N=2$  representation generated from it.

The following Lemma is an immediate result of direct calculations; we give it as a separate statement because it is often used in what follows.

**Lemma 3.3.** *The state  $|m\rangle_{bc} \otimes \gamma_{\lambda-1}^a |0\rangle_{\beta\gamma}$  satisfies the same highest-weight conditions as the twisted massive highest-weight vector  $|\frac{m+a}{p}, \frac{a(1-m)}{p}, p; -m\rangle$  if  $m \neq 0$ , and twisted topological highest-weight conditions (A.1) for  $m = 0$ :*

$$(3.22) \quad |m\rangle_{bc} \otimes \gamma_{\lambda-1}^a |0\rangle_{\beta\gamma} \doteq \begin{cases} \left| \frac{m+a}{p}, \frac{a(1-m)}{p}, p; -m \right\rangle, & m \in \mathbb{Z} \setminus \{0\}, \quad a \in \mathbb{N}, \\ \left| \frac{a+2}{p} - 1, p; -1 \right\rangle_{\text{top}}, & m = 0, \quad a \in \mathbb{N}. \end{cases}$$

Similarly,

$$(3.23) \quad |m\rangle_{bc} \otimes \beta_{-\lambda}^a |0\rangle_{\beta\gamma} \doteq \begin{cases} \left| \frac{m-a-2}{p} + 1, (a+1)(1 + \frac{m-2}{p}), p; 1-m \right\rangle, & m \in \mathbb{Z} \setminus \{1-p\}, \quad a \in \mathbb{N}, \\ \left| \frac{1-a}{p} - 1, p; p-1 \right\rangle_{\text{top}}, & m = 1-p, \quad a \in \mathbb{N}, \end{cases}$$

and also,

$$(3.24) \quad |m\rangle_{bc} \otimes |0\rangle_{\beta\gamma} \doteq \left| \frac{m}{p}, p; -m \right\rangle_{\text{top}}.$$

Now, if  $\widehat{\mathfrak{V}}_{\frac{1-r}{p}, p; r-1}(1-r, 0)$  were a true Verma module, we would have singular vectors (A.5) and (A.6),

$$(3.25) \quad |E(r, 1, p)\rangle^{+, r-1} = \mathcal{G}_{-1} \dots \mathcal{G}_{r-2} \left| \frac{1-r}{p}, p; r-1 \right\rangle_{\text{top}},$$

$$(3.26) \quad |E(p-r, 1, p)\rangle^{-, r-1} = \mathcal{Q}_{-p+1} \dots \mathcal{Q}_{-r} \left| \frac{1-r}{p}, p; r-1 \right\rangle_{\text{top}}.$$

**Lemma 3.4.** *In the  $N=2$  module  $\widehat{\mathfrak{V}}_{\frac{1-r}{p}, p; r-1}(1-r, 0)$  generated from vector (3.21), we have*

$$(3.27) \quad |E(r, 1, p)\rangle^{+, r-1} = 0,$$

$$(3.28) \quad |E(p-r, 1, p)\rangle^{-, r-1} = |1-p\rangle_{bc} \otimes \beta_{-\lambda}^{p-r} |0\rangle_{\beta\gamma}.$$

PROOF. Indeed, we write  $\mathcal{G}_j = \sum_{m \in \mathbb{Z} + \frac{1}{p}} (m - j\lambda) \gamma_{j-m} b_m$ , then

$$\mathcal{G}_{r-2} |1-r\rangle_{bc} \otimes |0\rangle_{\beta\gamma} = (1-\lambda)(r-1) b_{r-1-\lambda} |1-r\rangle_{bc} \otimes \gamma_{\lambda-1} |0\rangle_{\beta\gamma}$$

and further,  $\mathcal{G}_{r-3} \mathcal{G}_{r-2} |1-r\rangle_{bc} \otimes |0\rangle_{\beta\gamma}$  is in addition proportional to  $(1-\lambda)(r-2)$ , and so forth; therefore, singular vector (3.25) vanishes in  $\widehat{\mathfrak{V}}_{\frac{1-r}{p}, p; r-1}(1-r, 0)$ .  $\blacksquare$

Instead of the vanishing singular vector (3.25), the  $bc\beta\gamma$  representation space contains the vector

$$(3.29) \quad \begin{aligned} |C\rangle &= b_{-\lambda} \dots b_{r-2-\lambda} b_{r-1-\lambda} |1-r\rangle_{bc} \otimes \gamma_{\lambda-1}^r |0\rangle_{\beta\gamma} = |1\rangle_{bc} \otimes \gamma_{\lambda-1}^r |0\rangle_{\beta\gamma} \\ &\doteq \left| \frac{r+1}{p}, 0, p; -1 \right\rangle, \end{aligned}$$

from which the action of  $\mathcal{Q}$  produces the highest-weight vector:  $\mathcal{Q}_{-r+2} \dots \mathcal{Q}_0 \mathcal{Q}_1 |C\rangle = r! |1-r\rangle_{bc} \otimes |0\rangle_{\beta\gamma}$ . The module  $\widehat{\mathfrak{U}}_{\frac{r+1}{p}, 0, p; -1}(1, r)$  generated from  $|C\rangle$  has the vanishing charged singular vector

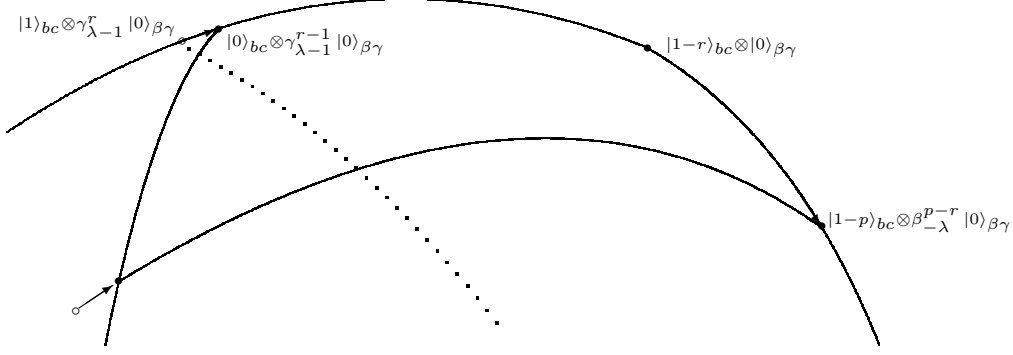


FIGURE 1. Topological highest-weight states and cosingular vectors on the extremal diagram. Filled dots denote the states satisfying twisted topological highest-weight conditions. The top parabola is the extremal diagram generated from the cosingular vector  $\circ$  (Eq. (3.29)), i.e., that of the  $\widehat{\mathfrak{U}}_{\frac{r+1}{p},0,p;-1}(1,r)$  module; the vanishing of the charged singular vector in  $\widehat{\mathfrak{U}}_{\frac{r+1}{p},0,p;-1}(1,r)$  results in the cusp at the state  $|1-r\rangle_{bc} \otimes |0\rangle_{\beta\gamma}$ . The submodule  $\widehat{\mathfrak{V}}_{\frac{1-r}{p},p;r-1}$  generated from  $|0\rangle_{bc} \otimes \gamma_{\lambda-1}^{r-1}|0\rangle_{\beta\gamma}$  is bounded by the “vertical” parabola. The lower parabola is the extremal diagram of the submodule built on singular vector (3.28).

$\mathcal{Q}_{1-r} \dots \mathcal{Q}_1 |\frac{r+1}{p}, 0, p; -1\rangle$ . Recalling the submodule  $\widehat{\mathfrak{V}}_{\frac{r+1}{p}-2,p;p-1}(1-p, r-p)$  generated from singular vector (3.28), we have the mappings

$$(3.30) \quad \widehat{\mathfrak{V}}_{\frac{r+1}{p}-2,p;p-1}(1-p, r-p) \xrightarrow{[\mathcal{Q}_{-p+1} \dots \mathcal{Q}_{-r}]} \widehat{\mathfrak{V}}_{\frac{1-r}{p},p;r-1}(1-r, 0) \xrightarrow{[\mathcal{Q}_{2-r} \dots \mathcal{Q}_0 \mathcal{Q}_1]} \widehat{\mathfrak{U}}_{\frac{r+1}{p},0,p;-1}(1, r),$$

where the square brackets in  $\mathfrak{A} \xrightarrow{[\mathcal{E}]} \mathfrak{B}$  indicate that the highest-weight vector of  $\mathfrak{A}$  is mapped onto the vector obtained by applying the operator  $\mathcal{E}$  to the highest-weight vector of  $\mathfrak{B}$ . It is useful to consider the extremal diagram [21] describing relations between the modules involved, see Figs. 1 and 2. The dotted line shows the extremal diagram of the *quotient* module  $\widehat{\mathfrak{U}}_{\frac{r+1}{p},0,p;-1}(1, r) / \widehat{\mathfrak{V}}_{\frac{1-r}{p},p;r-1}(1-r, 0)$ , in which the lower  $\circ$  state becomes the topological singular vector  $|E(p-r, 2, p)\rangle^{+,-1}$ .

The idea now is to observe that singular vector (3.28) is  $\mathbb{Q}_0$ -exact,

$$(3.31) \quad |1-p\rangle_{bc} \otimes \beta_{-\lambda}^{p-r} |0\rangle_{\beta\gamma} = a_{p,r} \mathbb{Q}_0 |2-p\rangle_{bc} \otimes \beta_{-\lambda}^{2p-r-1} |0\rangle_{\beta\gamma},$$

where  $a_{p,r}^{-1} = (p-r+1)(p-r+2) \dots (2p-r-1)$ ,<sup>4</sup> while vector (3.29) is not  $\mathbb{Q}_0$ -closed:

$$(3.32) \quad \mathbb{Q}_0 |1\rangle_{bc} \otimes \gamma_{\lambda-1}^r |0\rangle_{\beta\gamma} = |0\rangle_{bc} \otimes \gamma_{\lambda-1}^{p+r-1} |0\rangle_{\beta\gamma}.$$

As regards the highest-weight vector (3.21), further, we have

$$(3.33) \quad \mathbb{Q}_{\geq 1-r} |1-r\rangle_{bc} \otimes |0\rangle_{\beta\gamma} = 0,$$

in particular  $\mathbb{Q}_0 |1-r\rangle_{bc} \otimes |0\rangle_{\beta\gamma} = 0$ . Moreover,  $|1-r\rangle_{bc} \otimes |0\rangle_{\beta\gamma}$  is in the cohomology of  $\mathbb{Q}_0$  for  $1 \leq r \leq p-1$ , because the state  $|2-r\rangle_{bc} \otimes \beta_{-\lambda}^{p-1} |0\rangle_{\beta\gamma}$ , which is the candidate for the  $\mathbb{Q}_0$ -primitive of  $|1-r\rangle_{bc} \otimes |0\rangle_{\beta\gamma}$  according to the grading, would actually give the desired result only for  $r = p$ , which is outside the range of  $r$  for the *unitary* representations. In the cohomology of  $\mathbb{Q}_0$ , the singular vector

<sup>4</sup>In what follows, we omit similar factors, once we make sure they are nonzero.

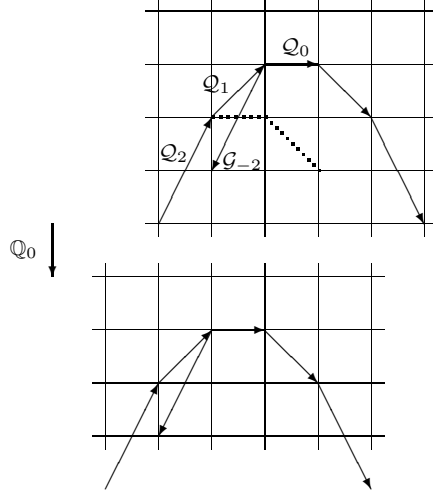


FIGURE 2. Extremal diagram near the cosingular vector and the mapping by  $\mathbb{Q}_0$ . The upper fragment is the top-left corner of Fig. 1 viewed through a magnifying glass. The cosingular vector is mapped by  $\mathbb{Q}_1$  into the module  $\widehat{\mathfrak{H}}_{\frac{1-r}{p}, p; r-1}$  generated by  $\dots, \mathcal{G}_{-2}, \mathbb{Q}_0, \mathbb{Q}_{-1}, \dots$ . The dotted line spanned by  $\mathbb{Q}_0 \mathbb{Q}_{-1} \dots$  is the extremal diagram of the corresponding quotient module. The lower diagram gives the result of applying  $\mathbb{Q}_0$ : in the target module, there is a *submodule* isomorphic to the quotient module shown in the dotted line, while the submodule from the upper diagram has vanished.

$|1-p\rangle_{bc} \otimes \beta_{-\lambda}^{p-r} |0\rangle_{\beta\gamma}$  in Fig. 1 vanishes. Since the cosingular vector, further, is *not* in the cohomology of  $\mathbb{Q}_0$ , this suggests that the cohomology is given precisely by the *unitary representation*  $\mathfrak{K}_{r,p;r-1}$ , which in terms of the *Verma* modules is given by (2.6).

We now make this argument more precise. Informally speaking, we have to show that although the submodule structure changes in the free-field realisation, the cohomology of  $\mathbb{Q}_0$  “effectively” performs the factorization similar to (2.6), and that there are no unwanted submodules in the cohomology. As regards the latter problem, it is easiest to carry over to the  $N=2$  setting the known results for the  $\widehat{\mathfrak{sl}}(2)$  modules in the Wakimoto bosonisation. We do this in the next subsection, and then return to the  $N=2$  analysis in Sec. 3.4.

**3.3. Mapping to the Wakimoto bosonisation.** We recall that the  $\widehat{\mathfrak{sl}}(2)$  currents can be constructed [19] from the  $N=2$  generators and a bosonic scalar field  $\chi$  such that  $\partial\chi(z)\partial\chi(w) = \frac{-1}{(z-w)^2}$ :

$$(3.34) \quad J^+ = \mathcal{Q} e^\chi, \quad J^0 = -\frac{p}{2} \mathcal{H} + \frac{p-2}{2} \partial\chi, \quad J^- = p \mathcal{G} e^{-\chi}.$$

These  $\widehat{\mathfrak{sl}}(2)_{p-2}$  generators commute with the current  $I^- = \sqrt{\frac{p}{2}}(\mathcal{H} - \partial\chi)$ . Applying this construction to the  $bc\beta\gamma$  realisation of the  $N=2$  algebra, we bosonise the fermionic ghosts as

$$(3.35) \quad b = e^{-\varphi}, \quad c = e^{\varphi},$$

and define a new first-order bosonic system and an independent current as

$$(3.36) \quad \beta = \beta e^{\chi+\varphi},$$

$$(3.37) \quad \gamma = \gamma e^{-\chi-\varphi},$$

$$(3.38) \quad \sqrt{\frac{p}{2}} \partial \varphi = -\frac{1}{2} \beta \gamma + \frac{p+1}{2} \partial \varphi + \frac{p}{2} \partial \chi.$$

In terms of these fields,  $\widehat{sl}(2)_{p-2}$  currents (3.34) take the Wakimoto form

$$(3.39) \quad \begin{aligned} J^+ &= -\beta, \\ J^0 &= \sqrt{p/2} \partial \varphi + \beta \gamma, \\ J^- &= \beta \gamma \gamma + \sqrt{2p} \gamma \partial \varphi + (p-2) \partial \gamma. \end{aligned}$$

Now, further bosonising the  $\beta \gamma$  fields from (3.4) as

$$(3.40) \quad \beta = \partial \xi e^{-\phi}, \quad \gamma = \eta e^{\phi},$$

where  $\eta \xi$  is a first-order fermionic system, we can construct the bosonic screening for the  $N=2$  generators (3.4):

$$(3.41) \quad S_W = \frac{1}{2\pi i} \oint \beta e^{\frac{1}{p}(\phi - \varphi)} = \frac{1}{2\pi i} \oint \partial \xi e^{(\frac{1}{p}-1)\phi - \frac{1}{p}\varphi}.$$

In terms of the new fields introduced in (3.36)–(3.38), this becomes the standard Wakimoto bosonisation screening (i.e., the one involved in the construction of the Felder-type resolution [4]):

$$(3.42) \quad S_W = \frac{1}{2\pi i} \oint \beta e^{-\sqrt{2/p} \varphi}.$$

Note that the  $\beta \gamma$  system pertaining to the Wakimoto representation is bosonised as  $\beta = \partial \xi e^{-\phi}$ ,  $\gamma = \eta e^{\phi}$  with the same  $\eta$  and  $\xi$  as in (3.40).

In terms of the Wakimoto bosonisation ingredients, the fermionic screening  $\mathbb{Q}_0$  becomes

$$(3.43) \quad \mathbb{Q}_0 = \frac{1}{2\pi i} \oint e^{\sqrt{2p} \varphi} \gamma^{p-1} e^{\phi}.$$

This involves the “constituent”  $\phi$  field in addition to the  $\beta \gamma$  fields as such. The complete bosonisation also gives rise to the second fermionic screening

$$(3.44) \quad \frac{1}{2\pi i} \oint \eta$$

that reduces the space of states by eliminating the  $\xi_0$  mode [18]. The most important point about the  $\mathbb{Q}_0$  screening in the  $\widehat{sl}(2)$  language is that it maps between  $\widehat{sl}(2)$  modules with different *twists* (i.e., the modules transformed by the spectral flow [19, 16]). This occurs because the  $e^{\phi}$  factor in (3.43) changes the  $\beta \gamma$  picture and hence the twist of the  $\widehat{sl}(2)$  highest-weight vector. Therefore, when applying the recipe of [19] to rewrite (3.18) in terms of  $\widehat{sl}(2)$  modules in the Wakimoto bosonisation, we obtain the resolution that “intersects” with the one known from [4, 5] at only one point, the “central” module, since all the other modules in the  $\widehat{sl}(2)$  analogue of (3.18) have non-zero twists. To avoid possible misunderstanding regarding how a *screening* changes the highest-weight conditions, we show in the next diagram several mappings, each of which is a counterpart of the one in Fig. 2 (with the extremal diagram conventions as in [19]; we also indicate the vertex operators corresponding to the highest-weight

vectors of the “untwisted” module (the one carrying the cohomology) and its submodule):

(3.45)

In the central and in the right module, a submodule is in the kernel of  $\mathbb{Q}_0$ ; the corresponding quotient module, whose extremal diagram is shown in the dotted line, is then mapped onto a submodule in the next module on the left:

(3.46) 
$$\begin{aligned} \beta^{p-r} e^{\frac{r-1}{\sqrt{2p}}\phi} &= \mathbb{Q}_0 \beta^{2p-r-1} e^{-\phi} e^{\frac{r-2p-1}{\sqrt{2p}}\phi}, \\ J_0^+ \beta^{2p-r-1} e^{-\phi} e^{\frac{r-2p-1}{\sqrt{2p}}\phi} &= \beta^{2p-r} e^{-\phi} e^{\frac{r-2p-1}{\sqrt{2p}}\phi} = \mathbb{Q}_0 \beta^{3p-r-1} e^{-2\phi} e^{\frac{r-4p-1}{\sqrt{2p}}\phi}, \\ J_1^+ \beta^{3p-r-1} e^{-2\phi} e^{\frac{r-4p-1}{\sqrt{2p}}\phi} &= \mathbb{Q}_0 (\dots). \end{aligned}$$

This pattern continues further right, where there is a sequence of Wakimoto modules with growing twists (i.e., transformed by the  $\widehat{sl}(2)$  spectral flow with  $\theta = 1, 2, \dots$ ). Thus, recalling the results of [4, 5] on the Wakimoto modules, we already know how the irreducible subquotients arrange in the  $N=2$  modules in  $\mathfrak{G}_{n,\nu,p}$ .<sup>5</sup> We now work out some details in the  $N=2$  language.

**3.4. End of the proof of Theorem 3.1.** We continue working with the  $\nu = 0$  case, Eq. (3.17). We observe that there are the following mappings that extend (3.31) (up to some nonzero factors, which can be easily restored):

(3.47) 
$$\begin{array}{ccc} |2-p\rangle_{bc} \otimes \beta_{-\lambda}^{3p-r-1} |0\rangle_{\beta\gamma} & \xrightarrow{\mathbb{Q}_{1-p}} & \dots \\ \downarrow \mathbb{Q}_0 & & \\ |2-p\rangle_{bc} \otimes \beta_{-\lambda}^{2p-r-1} |0\rangle_{\beta\gamma} & \xrightarrow{\mathbb{Q}_{1-p}} & |1-p\rangle_{bc} \otimes \beta_{-\lambda}^{2p-r} |0\rangle_{\beta\gamma} \\ \downarrow \mathbb{Q}_0 & & \\ |1-p\rangle_{bc} \otimes \beta_{-\lambda}^{p-r} |0\rangle_{\beta\gamma} & & \end{array}$$

Evaluating highest-weight conditions for the thus arising states  $|2-p\rangle_{bc} \otimes \beta_{-\lambda}^{mp-r-1} |0\rangle_{\beta\gamma}$  and  $|1-p\rangle_{bc} \otimes \beta_{-\lambda}^{mp-r} |0\rangle_{\beta\gamma}$ , we find

(3.48) 
$$|1-p\rangle_{bc} \otimes \beta_{-\lambda}^{mp-r} |0\rangle_{\beta\gamma} \doteq \left| \frac{r+1}{p} - m - 1, p; p-1 \right\rangle_{\text{top}}, \quad m = 1, 2, \dots$$

(3.49) 
$$\begin{aligned} |2-p\rangle_{bc} \otimes \beta_{-\lambda}^{mp-r-1} |0\rangle_{\beta\gamma} &\doteq \left| \frac{r+1}{p} - m, 0, p; p-1 \right\rangle, \\ &= \mathbb{Q}_{2-p} \dots \mathbb{Q}_{(m-1)p-r} |(m-1)p-r+1\rangle_{bc} \otimes |0\rangle_{\beta\gamma}, \end{aligned}$$

<sup>5</sup>As an aside, it would be interesting to construct, similarly to [5], the modules “interpolating” between the Verma modules entering the BGG resolution and the *twisted* Wakimoto modules from the  $\widehat{sl}(2)$  counterpart of (3.18).

where, further,  $|(m-1)p-r+1\rangle_{bc} \otimes |0\rangle_{\beta\gamma} \doteq |\frac{1-r}{p} + m-1, p; r-1-(m-1)p\rangle_{\text{top}}$ . For every  $m \in \mathbb{N}$ , therefore, we have a pair of modules

$$(3.50) \quad \widehat{\mathfrak{V}}_{\frac{1-r}{p}+m-1, p; r-1-(m-1)p}((m-1)p-r+1, 0) \supset \widehat{\mathfrak{V}}_{\frac{r+1}{p}-m-1, p; p-1}(1-p, r-mp)$$

(of course, the *modules* are mapped in the opposite directions to the  $\xrightarrow{\mathcal{Q}_{1-p}}$  arrows in (3.47)). The topological Verma module  $\mathfrak{V}_{\frac{1-r}{p}+m-1, p; r-1-(m-1)p}$  corresponding to the module on the left-hand side of (3.50) has singular vectors  $|E(pm-r, 1, p)\rangle^{-, r-1-(m-1)p}$  and  $|E(r, m, p)\rangle^{+, r-1-(m-1)p}$ . The first of these corresponds to the twisted topological Verma module  $\mathfrak{V}_{\frac{r+1}{p}-m-1, p; p-1}$ , and in the ghost realisation, indeed, evaluates as the highest-weight vector of the submodule on the right-hand side of (3.50). On the other hand,  $|E(r, m, p)\rangle^{+, r-1-(m-1)p}$  vanishes in  $\widehat{\mathfrak{V}}_{\frac{1-r}{p}+m-1, p; r-1-(m-1)p}((m-1)p-r+1, 0)$ .

Next, in the twisted topological Verma module built on the highest-weight state as on the right-hand side of (3.50), there are singular vectors  $|E((m+1)p-r, 1, p)\rangle^{+, p-1}$  and  $|E(r, m+1, p)\rangle^{-, p-1}$ . As regards the first one, we immediately see from (A.5) that it vanishes in the ghost realisation. To see what happens to the other one, we use the recursive nature of Eqs. (A.8) and (A.7). In  $\widehat{\mathfrak{V}}_{\frac{r+1}{p}-m-1, p; p-1}(1-p, r-mp)$ , singular vector (A.8) with the twist parameter  $\theta = p-1$  becomes

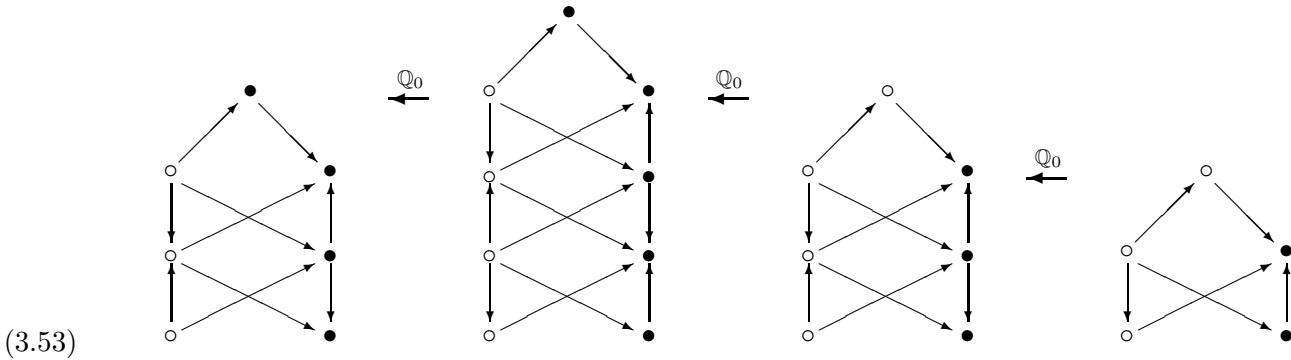
$$(3.51) \quad |E(r, m+1, p)\rangle^{-, p-1} = q(1-r-p, (m-1)p) \mathcal{E}^{+, r-(m-1)p-1}(r, m, p) \cdot q((m-1)p-r+1, -p) |1-p\rangle_{bc} \otimes \beta_{-\lambda}^{mp-r} |0\rangle_{\beta\gamma},$$

where we can *directly evaluate* the action of the continued operator  $q((m-1)p-r+1, -p)$  on the highest-weight state in the ghost realisation:

$$(3.52) \quad q((m-1)p-r+1, -p) |1-p\rangle_{bc} \otimes \beta_{-\lambda}^{mp-r} |0\rangle_{\beta\gamma} = |(m-1)p-r+1\rangle_{bc} \otimes |0\rangle_{\beta\gamma}.$$

It is essential here that the rest of the right-hand side of (3.51) contains only the operators from the universal enveloping of the  $N=2$  algebra, since  $q(1-r-p, (m-1)p) = \mathcal{Q}_{1-r-p} \dots \mathcal{Q}_{(m-1)p}$  in (3.51). Therefore, the singular vector in (3.51) is a descendant of  $|E(r, m, p)\rangle^{+, r-1-(m-1)p}$  and, thus, vanishes.

Continuing in this way, we obtain the two central diagrams (for  $m=1$  and 2) and the subsequent diagrams on the right in the sequence



which is continued to the left as we explain momentarily. The *submodule* represented by the filled dots in each diagram is the kernel of  $\mathcal{Q}_0$ . These diagrams show the “adjacency” of irreducible subquotients, as discussed after Eq. (A.9).

Now, this can be continued to the left of the center as follows. The module  $\widehat{\mathfrak{V}}_{\frac{1-r}{p}, p; r-1}(1-r, 0)$  can equivalently be written as  $\widehat{\mathfrak{V}}_{\frac{r+1}{p}-1, p; -1}(0, r-1)$ , which simply corresponds to taking the next cusp to the left on the extremal diagram as the highest-weight vector (see Fig. 1)  $|0\rangle_{bc} \otimes \gamma_{\lambda-1}^{r-1} |0\rangle_{\beta\gamma} \doteq \left| \frac{r+1}{p} - 1, p; -1 \right\rangle_{\text{top}}$ . As we have seen,  $\mathcal{Q}_1 |1\rangle_{bc} \otimes \gamma_{\lambda-1}^r |0\rangle_{\beta\gamma} = |0\rangle_{bc} \otimes \gamma_{\lambda-1}^{r-1} |0\rangle_{\beta\gamma}$ . This and Eq. (3.32) can now be continued as follows (again, up to nonvanishing factors):

$$\begin{aligned}
 & \begin{array}{ccc}
 & |1\rangle_{bc} \otimes \gamma_{\lambda-1}^r |0\rangle_{\beta\gamma} & \xrightarrow{\mathcal{Q}_1} |0\rangle_{bc} \otimes \gamma_{\lambda-1}^{r-1} |0\rangle_{\beta\gamma} \\
 & \downarrow \mathcal{Q}_0 & \\
 (3.54) \quad & |1\rangle_{bc} \otimes \gamma_{\lambda-1}^{p+r} |0\rangle_{\beta\gamma} & \xrightarrow{\mathcal{Q}_1} |0\rangle_{bc} \otimes \gamma_{\lambda-1}^{p+r-1} |0\rangle_{\beta\gamma} \\
 & \downarrow \mathcal{Q}_0 & \\
 & \dots \xrightarrow{\mathcal{Q}_1} |0\rangle_{bc} \otimes \gamma_{\lambda-1}^{2p+r-1} |0\rangle_{\beta\gamma}
 \end{array}
 \end{aligned}$$

We thus obtain the “gravitational descendants” of the highest-weight state,<sup>6</sup>

$$(3.55) \quad |0\rangle_{bc} \otimes \gamma_{\lambda-1}^{mp+r-1} |0\rangle_{\beta\gamma} \doteq \left| \frac{r+1}{p} + m - 1, p; -1 \right\rangle_{\text{top}}, \quad m = 0, 1, 2, \dots$$

From the twisted topological highest-weight conditions satisfied by these vectors, it follows, in particular, that the arrows  $\xrightarrow{\mathcal{Q}_1}$  cannot be inverted:  $\mathcal{G}_{-1} |0\rangle_{bc} \otimes \gamma_{\lambda-1}^{mp+r-1} = 0$ .

In each of the modules  $\widehat{\mathfrak{U}}_{\frac{r+1}{p}+m, 0, p; -1}$  generated from the states  $|1\rangle_{bc} \otimes \gamma_{\lambda-1}^{pm+r} |0\rangle_{\beta\gamma} \doteq \left| \frac{r+1}{p} + m, 0, p; -1 \right\rangle$  in (3.54), the charged singular vector  $\mathcal{Q}_{1-r-pm} \dots \mathcal{Q}_1 |1\rangle_{bc} \otimes \gamma_{\lambda-1}^{pm+r} |0\rangle_{\beta\gamma}$  vanishes. Each of these modules also has the charged singular vector  $\mathcal{Q}_1 \left| \frac{r+1}{p} + m, 0, p; -1 \right\rangle$ , the *quotient* over which is isomorphic to  $\widehat{\mathfrak{V}}_{\frac{r+1}{p}+m, p; -1}$ ; on the other hand, the *submodule* generated from the  $\mathcal{Q}_1$ -singular vector in the next module  $\widehat{\mathfrak{U}}_{\frac{r+1}{p}+m+1, 0, p; -1}$  is isomorphic to  $\widehat{\mathfrak{V}}_{\frac{r+1}{p}+m, p; -1}$  (see Fig. 2). Continuing in this way, we also recall that diagrams (3.54) and (3.47) are glued together as shown in Eq. (3.30),  $|0\rangle_{bc} \otimes \gamma_{\lambda-1}^{r-1} |0\rangle_{\beta\gamma} \xrightarrow{\mathcal{Q}_{1-p} \dots \mathcal{Q}_{-r} \mathcal{Q}_{2-r} \dots \mathcal{Q}_0} |1-p\rangle_{bc} \otimes \beta_{-\lambda}^{p-r} |0\rangle_{\beta\gamma}$ .

From the the “adjacency” structure of the irreducible subquotients, as described in (3.53), we immediately conclude that the cohomology is concentrated at one term and that it is the unitary representation  $\mathfrak{K}_{r,p}$ . ■

#### 4. THE “SYMMETRIC” REALISATION

**4.1. Generalities.** We now consider the realisation of the  $N=2$  algebra [11, 12, 13] that has the following form in the conventions corresponding to (2.1):

$$\begin{aligned}
 (4.1) \quad & \mathcal{G}(z) = C(z)A(z) - \partial C(z), \\
 & \mathcal{Q}(z) = B(z)\overline{A}(z) - \frac{1}{p}\partial B(z), \\
 & \mathcal{H}(z) = \overline{A}(z) - \frac{1}{p}A(z) - B(z)C(z), \\
 & \mathcal{T}(z) = \partial B(z)C(z) + \overline{A}(z)A(z) - \partial \overline{A}(z),
 \end{aligned}$$

<sup>6</sup>That the above diagram involves the mode  $\mathcal{Q}_1$  is in accordance with the spectral flow transform by  $\theta = -1$  of highest-weight states (3.55); twist 0 would correspond to  $\mathcal{Q}_0$ , and to  $\mathcal{Q}_{-p}$  in (3.47). Note also that by restoring the coefficients, we obtain (3.19).

where the free-field operator products are

$$(4.2) \quad \overline{A}(z) A(w) = \frac{1}{(z-w)^2}, \quad B(z) C(w) = \frac{1}{z-w}.$$

We call this realisation *symmetric* because the  $\mathcal{G}$  and  $\mathcal{Q}$  operators are expressed through the free fields in an essentially symmetric way, which is in contrast with the (inequivalent) “asymmetric” realisation [14, 15] of the  $N=2$  algebra. We expand into modes as  $A(z) = \sum_{n \in \mathbb{Z}} A_n z^{-n-1}$ ,  $\overline{A}(z) = \sum_{n \in \mathbb{Z}} \overline{A}_n z^{-n-1}$ , and  $B(z) = \sum_{n \in \mathbb{Z}} B_n z^{-n}$ ,  $C(z) = \sum_{n \in \mathbb{Z}} C_n z^{-n-1}$ .

**Lemma 4.1.** *The  $N=2$  spectral flow is induced by transforming the free fields entering (4.1) as follows:*

$$(4.3) \quad \begin{aligned} C_n &\mapsto C_{n+\theta}, & A_n &\mapsto A_n + \theta \delta_{n,0}, \\ B_n &\mapsto B_{n-\theta}, & \overline{A}_n &\mapsto \overline{A}_n - \frac{\theta}{p} \delta_{n,0}. \end{aligned}$$

PROOF. One only has to note that under this transformation, the composite  $BC$  operators acquire, in the standard way, a contribution coming from normal reordering (which is omitted from the notations),

$$(4.4) \quad (BC)_n \mapsto (BC)_n - \theta \delta_{n,0}, \quad (\partial B C)_n \mapsto (\partial B C)_n - \theta (BC)_n + \frac{\theta^2 + \theta}{2} \delta_{n,0}.$$

■

There are two fermionic screenings

$$(4.5) \quad S_B = \frac{1}{2\pi i} \oint B e^X, \quad S_C = \frac{1}{2\pi i} \oint C e^{p\overline{X}},$$

where  $\partial X = A$  and  $\partial \overline{X} = \overline{A}$ . Note that, obviously, the screenings are unchanged under (4.3).

We now introduce modules over these free fields.  $\Lambda = \Lambda_0(0)$  is the  $BC$  module generated from  $|0\rangle_{BC}$  (see (3.9) and (3.11), where now  $\lambda = 0$ ); next, let the state  $|\overline{a}, a\rangle_{\overline{A}A}$  be such that

$$(4.6) \quad \overline{A}_0 |\overline{a}, a\rangle_{\overline{A}A} = \overline{a} |\overline{a}, a\rangle_{\overline{A}A}, \quad A_0 |\overline{a}, a\rangle_{\overline{A}A} = a |\overline{a}, a\rangle_{\overline{A}A},$$

$$(4.7) \quad \overline{A}_{\geq 1} |\overline{a}, a\rangle_{\overline{A}A} = A_{\geq 1} |\overline{a}, a\rangle_{\overline{A}A} = 0$$

and let  $\mathfrak{H}_{\overline{a},a}$  be the Fock module generated from  $|\overline{a}, a\rangle_{\overline{A}A}$ . We define the ghost representation space

$$(4.8) \quad \mathbb{G}_{r,p} = \Lambda \otimes \bigoplus_{m,n \in \mathbb{Z}} \mathfrak{H}_{n,mp+r-1}.$$

It is in this space that we will identify the unitary representation  $\mathfrak{K}_{r,p;0}$ . The other  $\mathfrak{K}_{r,p;\theta}$  then follow by applying the spectral flow transform in accordance with (4.3).

*Notation for the  $N=2$  modules.* Similarly to the conventions used in Sec. 3.2, we denote the module generated from  $|M\rangle_{BC} \otimes |\overline{a}, a\rangle_{\overline{A}A} \in \mathbb{G}_{r,p}$  by  $\widetilde{\mathfrak{U}}_{h,\ell,p;\theta}(M, \overline{a}, a)$  whenever  $|M\rangle_{BC} \otimes |\overline{a}, a\rangle_{\overline{A}A} \doteq |h, \ell, p; \theta\rangle$  (i.e., the state satisfies twisted massive highest-weight conditions (A.10)–(A.12)), and by  $\widetilde{\mathfrak{V}}_{h,p;\theta}(M, \overline{a}, a)$  in the case where  $|M\rangle_{BC} \otimes |\overline{a}, a\rangle_{\overline{A}A} \doteq |h, p; \theta\rangle_{\text{top}}$ . We will sometimes omit the  $(M, \overline{a}, a)$  arguments, explicitly indicating instead the vector(s) from which the module is generated. Note, however, that there will also appear  $N=2$  modules that are not generated from a single vector.



In  $\mathbb{G}_{r,p}$ , we take the state  $|0\rangle_{BC} \otimes |0, r-1\rangle_{\overline{AA}}$  which satisfies the (twist-zero) topological highest-weight conditions with respect to  $N=2$  generators (4.1):

$$(4.9) \quad |0\rangle_{BC} \otimes |0, r-1\rangle_{\overline{AA}} \doteq \left| \frac{1-r}{p}, p \right\rangle_{\text{top}}.$$

**4.2. The butterfly resolution.** Let  $\tilde{\mathfrak{Y}}_{\frac{1-r}{p}, p}(0, 0, r-1)$  be the  $N=2$  module generated from (4.9). It is a submodule in the “central” term  $\odot$  (the one carrying the cohomology) in the *butterfly resolution*:<sup>7</sup>

$$(4.10) \quad \begin{array}{c} \vdots \quad \vdots \quad \vdots \\ \leftarrow S_C \bullet \xleftarrow{S_C} \bullet \xleftarrow{S_C} \bullet \\ \uparrow S_B \quad \uparrow S_B \quad \uparrow S_B \\ \leftarrow S_C \bullet \xleftarrow{S_C} \bullet \xleftarrow{S_C} \bullet \\ \uparrow S_B \quad \uparrow S_B \quad \uparrow S_B \\ \leftarrow S_C \bullet \xleftarrow{S_C} \bullet \xleftarrow{S_C} \odot \\ \uparrow S_B \quad \uparrow S_B \quad \uparrow S_B \\ \vdots \quad \vdots \quad \vdots \end{array} \quad \begin{array}{c} \bullet \xleftarrow{S_C} \bullet \xleftarrow{S_C} \bullet \quad \dots \\ \uparrow S_B \quad \uparrow S_B \quad \uparrow S_B \\ \bullet \xleftarrow{S_C} \bullet \xleftarrow{S_C} \bullet \quad \dots \\ \uparrow S_B \quad \uparrow S_B \quad \uparrow S_B \\ \bullet \xleftarrow{S_C} \bullet \xleftarrow{S_C} \bullet \quad \dots \\ \uparrow S_B \quad \uparrow S_B \quad \uparrow S_B \\ \vdots \quad \vdots \quad \vdots \end{array}$$

On the right wing, the modules are  $\tilde{\mathfrak{Y}}_{\frac{r+1}{p} - n - m, 0, p; np - r}(np - r, -m, r - np - 1)$ , which are labeled by positive integers  $m$  and  $n$ , where  $n$  labels columns (with  $n = 1$  for the left column) and  $m$  labels rows (with  $m = 1$  for the top row). On the left wing, the construction is “dual” in the obvious sense (the arrows reversed), the modules are labeled by nonnegative integers  $m$  and  $n$ , with  $m = 0$  for the bottom row and  $n = 0$  for the right column, the  $(m, n)$  module being the result of gluing together the modules generated from the states  $|-r - np\rangle_{BC} \otimes |m, np + r - 1\rangle_{\overline{AA}}$  and  $|mp + 1\rangle_{BC} \otimes |m, np + r - 1\rangle_{\overline{AA}}$ . In particular, the  $\odot$ -module is obtained by gluing together the  $N=2$  modules generated from  $|-r\rangle_{BC} \otimes |0, r-1\rangle_{\overline{AA}}$  and from  $|1\rangle_{BC} \otimes |0, r-1\rangle_{\overline{AA}}$ , which have a common submodule generated from (4.9).

**Theorem 4.2.** *Diagram (4.10) consisting of  $N=2$  representations on  $\mathbb{G}_{r,p}$  is exact except at the  $\odot$  module generated from the vectors  $|-r\rangle_{BC} \otimes |0, r-1\rangle_{\overline{AA}}$  and  $|1\rangle_{BC} \otimes |0, r-1\rangle_{\overline{AA}}$ , where the cohomology is given by the unitary  $N=2$  representation  $\mathfrak{K}_{r,p}$ .*

<sup>7</sup>Or rather a *sand-glass*, if rotated by  $135^\circ$ .

**Remark 4.3.** We have selected an  $r$  from the range  $1 \leq r \leq p-1$  arbitrarily, and defined the space  $\mathbb{G}_{r,p}$  depending on  $r$ . If we define

$$(4.11) \quad \mathbb{G}_{*,p} = \Lambda \otimes \bigoplus_{m,n \in \mathbb{Z}} \mathfrak{H}_{n,m},$$

the cohomology on this space is  $\bigoplus_{r=1}^{p-1} \mathfrak{K}_{r,p}$ .

**Remark 4.4.** The  $N=2$  spectral flow acts on the states from  $\mathbb{G}_{*,p}$  according to

$$(4.12) \quad |n\rangle_{BC} \otimes |\bar{a}, a\rangle_{\overline{AA}} \mapsto |n+\theta\rangle_{BC} \otimes \left| \bar{a} + \frac{\theta}{p}, a - \theta \right\rangle_{\overline{AA}}.$$

This allows us to apply the spectral flow to the data in Theorem 4.2 (with  $\mathbb{G}_{r,p}$  mapping appropriately) in order to obtain all the unitary representations  $\mathfrak{K}_{r,p;\theta}$  from Sec. 2. Without a loss of generality, therefore, we work with a particular twist—and, thus, with the above  $\mathbb{G}_{r,p}$  space—as fixed by the choice made in (4.9).

PROOF. The construction of the resolution is based on charged singular vectors (A.14) and on the topological singular vectors (A.5) and (A.6) (those with  $s=1$ ). In the free-field realisation, these singular vectors may vanish, in which case we may find cosingular vectors in the same grade; if, on the other hand, the singular vector does not vanish, we consider the corresponding submodule and find similar singular vectors in it. Thus, for the state (4.9) and for other highest-weight states appearing on the way, we determine their annihilation conditions; these would be either twisted topological highest-weight conditions (A.1) or only twisted massive highest-weight conditions (A.11). We then evaluate the eigenvalues of the appropriate Cartan generators (using (A.2), (A.3), or (A.11)), look for the singular vectors, and investigate which (sub)modules are in the image or in the kernel of the screening operators; the action of the screenings on states from  $\mathbb{G}_{r,p}$  is evaluated via elementary conformal field theory calculations.

The middle. We begin with (4.9) and the corresponding  $N=2$  module  $\widetilde{\mathfrak{V}}_{\frac{1-r}{p},p}(0,0,r-1)$ . Evaluating the singular vector  $|E(r,1,p)\rangle^+$  (see (A.4)–(A.5)) in this module, we see that it vanishes. Because of this vanishing, the state  $|1-r\rangle_{BC} \otimes |0,r-1\rangle_{\overline{AA}}$  satisfies twisted *topological* highest-weight conditions:

$$(4.13) \quad |1-r\rangle_{BC} \otimes |0,r-1\rangle_{\overline{AA}} \doteq \left| \frac{r+1}{p} - 1, p; -r \right\rangle_{\text{top}}.$$

We now observe that vector (4.13) is in the image of  $S_B$ :

$$|1-r\rangle_{BC} \otimes |0,r-1\rangle_{\overline{AA}} = S_B | -r \rangle_{BC} \otimes | -1, r-1 \rangle_{\overline{AA}},$$

where we find  $| -r \rangle_{BC} \otimes | -1, r-1 \rangle_{\overline{AA}} \doteq \left| \frac{r+1}{p} - 1, 0, p; -r \right\rangle$ . In the module  $\widetilde{\mathfrak{U}}_{\frac{r+1}{p}-1,0,p;-r}$  generated from  $| -r \rangle_{BC} \otimes | -1, r-1 \rangle_{\overline{AA}}$ , there is a charged singular vector

$$(4.14) \quad \begin{aligned} \mathcal{G}_{-p} \dots \mathcal{G}_{-r-1} | -r \rangle_{BC} \otimes | -1, r-1 \rangle_{\overline{AA}} &= | -p \rangle_{BC} \otimes | -1, r-1 \rangle_{\overline{AA}} \\ &= S_C | 1-p \rangle_{BC} \otimes | -1, r-p-1 \rangle_{\overline{AA}}. \end{aligned}$$

The thus arising vector  $|1-p\rangle_{BC} \otimes |-1, r-p-1\rangle_{\overline{AA}}$  generates the module  $\widetilde{\mathfrak{U}}_{\frac{r+1}{p}-2,0,p;p-r}(p-r, -1, r-p-1)$ , which is the  $(m=1, n=1)$  case of the modules filling the right wing, as we describe momentarily. Note that we could equally well have arrived at the same module by first noticing that  $|0\rangle_{BC} \otimes |0, r-1\rangle_{\overline{AA}} = S_C |1\rangle_{BC} \otimes |0, r-p-1\rangle_{\overline{AA}}$ , where, further,  $\mathcal{Q}_{r-p} \dots \mathcal{Q}_{-1} |1\rangle_{BC} \otimes |0, r-p-1\rangle_{\overline{AA}} = |p-r+1\rangle_{BC} \otimes |0, r-p-1\rangle_{\overline{AA}} = S_B |p-r\rangle_{BC} \otimes |-1, r-p-1\rangle_{\overline{AA}}$ , with  $|p-r\rangle_{BC} \otimes |-1, r-p-1\rangle_{\overline{AA}}$  and  $|1-p\rangle_{BC} \otimes |-1, r-p-1\rangle_{\overline{AA}}$  being descendants of each other. This defines the central arrow in (4.10) as  $S_B \circ S_C$ , which equals  $S_C \circ S_B$  up to the (irrelevant) sign.

The right wing. Assigning  $n=1$  to the left column and  $m=1$  to the top row, the module in column  $n$  and line  $m$  is given by

$$(4.15) \quad \begin{aligned} \widetilde{\mathfrak{U}}_{\frac{r+1}{p}-n-m,0,p;np-r}(np-r, -m, r-np-1) = \\ = \widetilde{\mathfrak{U}}_{n+m-\frac{r+1}{p}, n+m-\frac{r+1}{p}, p; 1-mp}(1-mp, -m, r-np-1), \end{aligned}$$

which can be generated from any of the vectors

$$|np-r\rangle_{BC} \otimes |-m, r-np-1\rangle_{\overline{AA}} \doteq \left| \frac{r+1}{p} - m - n, 0, p; np-r \right\rangle$$

or

$$|1-mp\rangle_{BC} \otimes |-m, r-np-1\rangle_{\overline{AA}} \doteq \left| n+m-\frac{r+1}{p}, n+m-\frac{r+1}{p}, p; 1-mp \right\rangle.$$

We first note that the equality in (4.15) occurs in view of the relations

$$\begin{aligned} \mathcal{Q}_{-np+r+1} \dots \mathcal{Q}_{mp-1} |1-mp\rangle_{BC} \otimes |-m, r-np-1\rangle_{\overline{AA}} &= |np-r\rangle_{BC} \otimes |-m, r-np-1\rangle_{\overline{AA}} \\ |1-mp\rangle_{BC} \otimes |-m, r-np-1\rangle_{\overline{AA}} &= \mathcal{G}_{1-mp} \dots \mathcal{G}_{np-r-1} |np-r\rangle_{BC} \otimes |-m, r-np-1\rangle_{\overline{AA}} \end{aligned}$$

(which hold up to *nonvanishing* factors), and therefore, the states  $|1-mp\rangle_{BC} \otimes |-m, r-np-1\rangle_{\overline{AA}}$  and  $|np-r\rangle_{BC} \otimes |-m, r-np-1\rangle_{\overline{AA}}$  generate the same module.

Next, a simple calculation shows that there are the following charged singular vectors in the module in Eq. (4.15):

$$\begin{array}{ll} \mathcal{G}_{-mp} |1-mp\rangle_{BC} \otimes |-m, r-np-1\rangle_{\overline{AA}} \in \widetilde{\mathfrak{U}}_{\frac{r+1}{p}-m-n,0,p;np-r} \ni \mathcal{Q}_{r-np} |np-r\rangle_{BC} \otimes |-m, r-np-1\rangle_{\overline{AA}} & \\ \parallel & \parallel \\ |-mp\rangle_{BC} \otimes |-m, r-np-1\rangle_{\overline{AA}} & |1+np-r\rangle_{BC} \otimes |-m, r-np-1\rangle_{\overline{AA}} \\ \parallel \cdot & \parallel \cdot \\ |n+m+\frac{1-r}{p}, p; -mp\rangle_{\text{top}} & \left| \frac{r+1}{p} - n - m - 1, p; np-r \right\rangle_{\text{top}} \\ \parallel & \parallel \\ S_C |1-mp\rangle_{BC} \otimes |-m, r-(n+1)p-1\rangle_{\overline{AA}} & S_B |np-r\rangle_{BC} \otimes |-m-1, r-np-1\rangle_{\overline{AA}} \end{array}$$

Evaluating the annihilation and eigenvalue conditions satisfied by  $|1-mp\rangle_{BC} \otimes |-m, r-(n+1)p-1\rangle_{\overline{AA}}$  and  $|np-r\rangle_{BC} \otimes |-m-1, r-np-1\rangle_{\overline{AA}}$ , we see that the same steps as above apply to the modules generated from these vectors: each of these modules has two charged singular vectors, which are precisely in the image of one of the screenings. The “cross” combination of two screenings follows by repeating

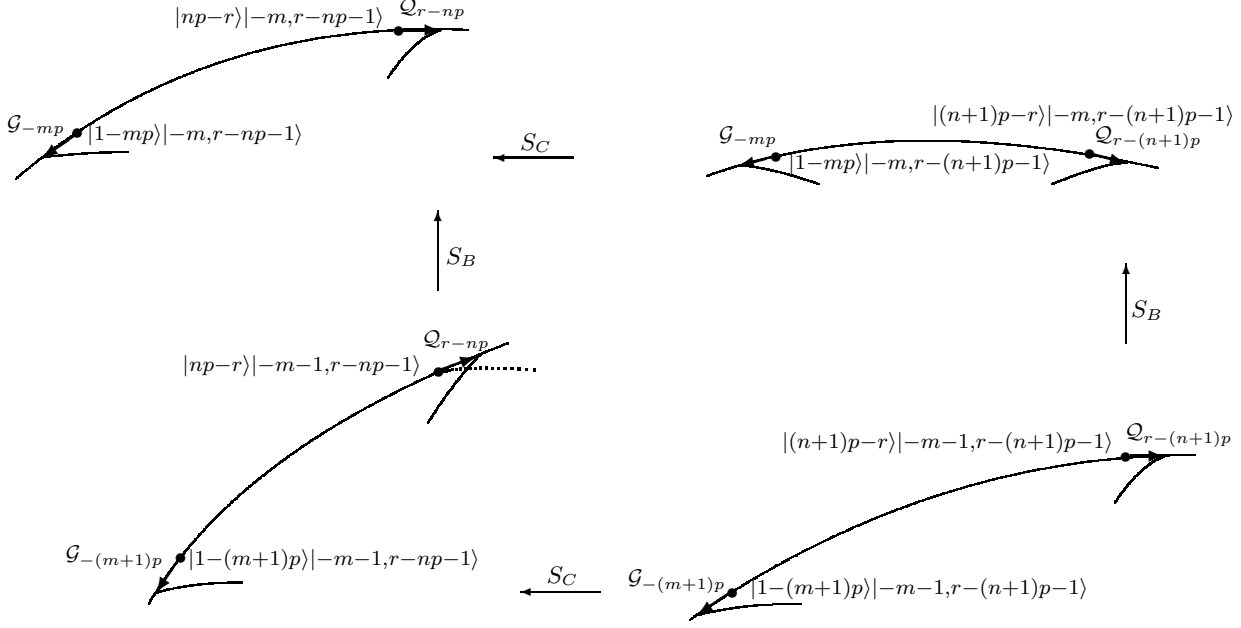


FIGURE 3. Extremal diagrams of modules mapped by the screening operators. For brevity, we omit the tensor product sign and the subscripts pertaining to different ket-vectors. Charged singular vectors and the corresponding submodules are shown as explained in (A.15). The filled dots show the states that are *mapped into* the charged singular vectors by the screenings. The dotted line shows in one case (and can be similarly drawn in other cases) the extremal diagram of the quotient module over the corresponding singular vector. The corresponding submodule being in the kernel of the screening, the dotted line is mapped onto the submodule extremal diagram in the target module.

the above calculations twice more. This can be best explained by Fig. 3, the outcome being that there exist the mappings

$$\begin{array}{ccccc}
 \vdots & & \vdots & & \vdots \\
 \uparrow S_B & & \uparrow S_B & & \uparrow S_B \\
 \cdots \xleftarrow{S_C} \widetilde{\mathfrak{U}}_{\frac{r+1}{p}-n-m,0,p;np-r} & \xleftarrow{S_C} & \widetilde{\mathfrak{U}}_{\frac{r+1}{p}-n-m-1,0,p;(n+1)p-r} & \xleftarrow{S_C} & \cdots \\
 \uparrow S_B & & \uparrow S_B & & \uparrow S_B \\
 \cdots \xleftarrow{S_C} \widetilde{\mathfrak{U}}_{\frac{r+1}{p}-n-m-1,0,p;np-r} & \xleftarrow{S_C} & \widetilde{\mathfrak{U}}_{\frac{r+1}{p}-n-m-2,0,p;(n+1)p-r} & \xleftarrow{S_C} & \cdots \\
 \uparrow S_B & & \uparrow S_B & & \uparrow S_B \\
 \vdots & & \vdots & & \vdots
 \end{array}
 \tag{4.16}$$

which constitute the pattern filling the right wing of the butterfly.

The left wing. We label the modules on the left wing by nonnegative integers  $m$  and  $n$ , with  $m = 0$  for the bottom line and  $n = 0$  for the vertical border. The  $(m, n)$  module is obtained by gluing together the modules generated from

$$\tag{4.17} \quad |-r-np\rangle_{BC} \otimes |m, np+r-1\rangle_{\overline{AA}} \doteq \left| \frac{r+1}{p} + m + n, 0, p; -r-np \right\rangle$$

and

$$(4.18) \quad |mp+1\rangle_{BC} \otimes |m, np+r-1\rangle_{\overline{AA}} \doteq \left| -\frac{r+1}{p} - m - n, -\frac{r+1}{p} - m - n, p; mp+1 \right\rangle.$$

*Gluing* refers to the fact that in the module generated from (4.17), there is a submodule generated from the singular vector

$$(4.19) \quad \begin{aligned} \mathcal{Q}_{r+np} | -r - np \rangle_{BC} \otimes |m, np+r-1\rangle_{\overline{AA}} &= |1-r-np\rangle_{BC} \otimes |m, np+r-1\rangle_{\overline{AA}} \\ &\doteq \left| \frac{r+1}{p} + m + n - 1, p; -r - np \right\rangle_{\text{top}}, \end{aligned}$$

and *the same* submodule is also generated from the singular vector

$$(4.20) \quad \mathcal{G}_{mp} |mp+1\rangle_{BC} \otimes |m, np+r-1\rangle_{\overline{AA}} = |mp\rangle_{BC} \otimes |m, np+r-1\rangle_{\overline{AA}}$$

in the module generated from (4.18), because the states  $|1-r-np\rangle_{BC} \otimes |m, np+r-1\rangle_{\overline{AA}}$  and  $|mp\rangle_{BC} \otimes |m, np+r-1\rangle_{\overline{AA}}$  are descendants of each other. Now, applying the screening operators, we have

$$(4.21) \quad \begin{aligned} S_B | -r - np \rangle_{BC} \otimes |m, np+r-1\rangle_{\overline{AA}} &= |1-r-np\rangle_{BC} \otimes |m+1, np+r-1\rangle_{\overline{AA}} \\ &= \mathcal{Q}_{r+np} | -r - np \rangle_{BC} \otimes |m+1, np+r-1\rangle_{\overline{AA}} \end{aligned}$$

and

$$(4.22) \quad \begin{aligned} S_C |mp+1\rangle_{BC} \otimes |m, np+r-1\rangle_{\overline{AA}} &= |mp\rangle_{BC} \otimes |m, (n+1)p+r+1\rangle_{\overline{AA}} \\ &= \mathcal{G}_{mp} |1+mp\rangle_{BC} \otimes |m, (n+1)p+r+1\rangle_{\overline{AA}}, \end{aligned}$$

which shows that the pattern (4.17)–(4.20) is reproduced in (4.21) and (4.22) with  $m \mapsto m+1$  and  $n \mapsto n+1$ , respectively. In the module generated from (4.17) *and* (4.18), further,  $\text{Ker } S_B$  is generated from (4.18), and  $\text{Ker } S_C$  from (4.17), while  $\text{Ker } S_B \cap \text{Ker } S_C$  is the submodule generated from (4.19). In this way, the entire left wing is filled (in the way that is in the obvious sense dual to the pattern on the right wing).

We now recall the standard fact that each horizontal or vertical sequence of mappings by *one* fermionic screening represented as a *vertex operator* is exact (except, obviously, at the border of the wing, if the sequence is continued as  $\dots \rightarrow 0$  or  $0 \rightarrow \dots$ ). Thus, the mappings are exact everywhere except at the corner. Next, the central mapping is given by the product of two screenings, and the cohomology can be worked out starting from the observation that  $\text{Im } S_B = \text{Im } S_C = \widetilde{\mathfrak{V}}_{\frac{1-r}{p}, p}(0, 0, r-1)$ , while  $\text{Im } S_B \circ S_C$  is the maximal submodule in  $\widetilde{\mathfrak{V}}_{\frac{1-r}{p}, p}(0, 0, r-1)$ . A more economical way to arrive at the same result is to map the butterfly resolution onto the two-sided resolution (3.18) as described in the next subsection. ■

**4.3. Jamming the butterfly into the two-sided resolution.** It is a reformulation of the fact known since [18] that taking the kernel or the cokernel of the fermionic screening gives rise to a  $\beta\gamma$  system. We apply this to the butterfly resolution, and then the resulting  $\beta\gamma$  system will be that of Sec. 3 (with the butterfly resolution becoming the “linear” two-sided resolution (3.18)). Indeed, since  $Ce^{p\overline{X}}$  in (4.5) is a fermion, we define

$$(4.23) \quad \eta = C e^{p\overline{X}}, \quad \xi = B e^{-p\overline{X}}$$

and also introduce two scalars  $\phi$  and  $\varphi$  with signatures  $-1$  and  $+1$ , respectively:

$$(4.24) \quad \partial\phi = BC + \frac{1}{p}A - p\bar{A}, \quad \partial\varphi = BC + \frac{1}{p}A.$$

The latter represents a fermionic ghost system  $bc$  constructed as in (3.35). Further, with  $\eta$ ,  $\xi$ , and  $\phi$  from (4.23)–(4.24), we introduce a first-order bosonic system in accordance with (3.40). Then the  $N=2$  generators (4.1) can be rewritten in terms of these  $(b, c, \beta, \gamma)$  fields as

$$(4.25) \quad \mathcal{Q} = -\frac{1}{p}\beta c, \quad \mathcal{G} = (p-1)b\partial\gamma - \gamma\partial b,$$

which differ from the respective generators in (3.4) only by  $\mathcal{Q} \mapsto p\mathcal{Q}$ ,  $\mathcal{G} \mapsto \frac{1}{p}\mathcal{G}$ , which does not change the commutation relations (the rest of the algebra is *generated by*  $\mathcal{Q}$  and  $\mathcal{G}$ ). Now the screening  $S_C$  becomes simply  $\eta_0$ , which “reduces” the  $\eta\xi\phi$  space of states to the  $\beta\gamma$  space of states by eliminating the  $\xi_0$  mode.

The other fermionic screening then becomes  $S_B = \frac{1}{2\pi i} \oint c\gamma^{p-1}$ , which is  $\mathbb{Q}_0$  from Sec. 3.

Now, the butterfly resolution can be mapped onto the two-sided resolution (3.18). This goes by “destroying” the wings such that only the  $S_B$  mappings remain. Consider first the right wing. We keep only the vertical border (see (4.10)): setting  $n = 1$  in (4.15), we are left with the mappings

$$(4.26) \quad \tilde{\mathfrak{U}}_{\frac{r+1}{p}-m-1,0,p;p-r}(p-r, -m, r-p-1) \xrightarrow{S_B} \tilde{\mathfrak{U}}_{\frac{r+1}{p}-m,0,p;p-r}(p-r, -m+1, r-p-1).$$

In each module, we now take the quotient over the image of  $S_C$ . As we have noted, this leaves us with the  $bc\beta\gamma$  representation space (i.e., the cohomology of  $0 \xleftarrow{S_C} \dots \xleftarrow{S_C} \dots$ ). On the other hand, the image of  $S_C$  is the submodule in  $\tilde{\mathfrak{U}}_{\frac{r+1}{p}-m-1,0,p;p-r}(p-r, -m, r-p-1)$  generated from

$$(4.27) \quad |-mp\rangle_{BC} \otimes |-m, r-p-1\rangle_{\bar{A}A} \doteq \left| \frac{1-r}{p} + m, p; -p \right\rangle_{\text{top}}.$$

The quotient module is then generated from

$$(4.28) \quad |1-mp\rangle_{BC} \otimes |-m, r-p-1\rangle_{\bar{A}A} \doteq \left| \frac{1-r}{p} + m, p; -mp \right\rangle_{\text{top}}$$

(where  $\doteq$  holds in the quotient, i.e. modulo the vector (4.27)). This gives the mappings

$$(4.29) \quad \dots \xrightarrow{S_B} \widehat{\mathfrak{V}}_{\frac{1-r}{p}+m+1,p;-(m+1)p}(1-(m+1)p, -m-1, r-p-1) \xrightarrow{S_B} \\ \xrightarrow{S_B} \widehat{\mathfrak{V}}_{\frac{1-r}{p}+m,p;-mp}(1-mp, -m, r-p-1) \xrightarrow{S_B} \dots \xrightarrow{S_B} \widehat{\mathfrak{V}}_{\frac{1-r}{p}+1,p;0}(1-p, -1, r-p-1),$$

where  $\widehat{\mathfrak{V}}$  are the modules in which the singular vector  $\mathcal{G}_{-mp}|1-mp\rangle_{BC} \otimes |-m, r-p-1\rangle_{\bar{A}A}$  (see the top-left extremal diagram in Fig. 3) has been factored over.

On the left wing, we take the modules on the vertical border ( $n = 0$  in (4.17)–(4.18)) and keep only the kernel of  $S_C$  (again, the cohomology of  $0 \xrightarrow{S_C} \dots \xrightarrow{S_C} \dots$ ). The kernel of  $S_C$  is generated from

$$(4.30) \quad |-r\rangle_{BC} \otimes |m, r-1\rangle_{\bar{A}A} \doteq \left| \frac{r+1}{p} + m, 0, p; -r \right\rangle, \quad m \geq 0$$

Denoting this module by  $\widehat{\mathfrak{U}}_{m+\frac{r+1}{p},0,p;-r}(-r, m, r-1)$ , we see that mappings (4.29) are continued as

$$(4.31) \quad \widehat{\mathfrak{U}}_{\frac{r+1}{p},0,p;-r}(-r, 0, r-1) \xrightarrow{S_B} \widehat{\mathfrak{U}}_{\frac{r+1}{p}+1,0,p;-r}(-r, 1, r-1) \xrightarrow{S_B} \widehat{\mathfrak{U}}_{\frac{r+1}{p}+2,0,p;-r}(-r, 2, r-1) \xrightarrow{S_B} \dots$$

We, thus, reproduce (3.18) transformed by the overall spectral flow with  $\theta = 1 - r$ .

**Remark 4.5.** Note that the *bosonic* screening of the  $N=2$  realisation (4.1), which reads as

$$(4.32) \quad S_W = \frac{1}{2\pi i} \oint (p\overline{A} - BC)e^{-\frac{1}{p}X - \overline{X}},$$

now takes the form (3.41); it is *not* involved in the resolutions considered in this paper.

Under a further mapping to the Wakimoto representation, as we have seen, the screening  $S_C = \frac{1}{2\pi i} \oint \eta$ , as before, serves to correctly define the representation space of the first-order bosonic system, now of the  $\beta\gamma$  system (thus, this screening becomes redundant as soon as one deals with the  $\beta$  and  $\gamma$  fields as such, rather than with their bosonisation). On the other hand, as we have seen, the fermionic screening  $S_B$  takes the form (3.43) (note that the screenings finally take the “standard” vertex-operator form).

## 5. CONCLUSIONS

We have constructed the two-sided “linear” resolution and the butterfly resolution of the unitary  $N=2$  representations. The resolutions show a “strong dependence” on the free-field realisation chosen (moreover, the “asymmetric” realisation [14, 15] of the  $N=2$  algebra shows yet different resolution structures [34]). In fact, it is the quantum group encoded in the structure of the screenings that determines the resolution. In the  $bc\beta\gamma$  bosonisation of the  $N=2$  algebra, we have seen (Theorem 3.1) to what extent the folklore statement that “the cohomology is generated from chiral primary fields” is true: the cohomology does contain a chiral primary state (the topological highest-weight states as we call them here) for each  $r$  from  $1 \leq r \leq p-1$ , however these, on the one hand, can also be *twisted* by the spectral flow, and on the other hand, have to correspond to a very particular irreducible subquotient in (3.53) (where infinitely many other twisted topological highest-weight states are *not* in the cohomology).

As regards the butterfly resolution, its shape can be heuristically interpreted as a “Felder-type” effect occurring in the “3, 5, 7, ...”-resolution of irreducible  $N=2$  representations [16]. The latter is constructed in terms of twisted *massive* Verma modules and goes like

$$(5.1) \quad \begin{array}{ccccccc} & & & & \bullet & & \\ & & & & \bullet & & \\ & & & \bullet & \bullet & & \\ 0 & \leftarrow & \bullet & \leftarrow & \bullet & \leftarrow & \bullet & \leftarrow \dots \\ & & & \bullet & \bullet & & \\ & & & \bullet & \bullet & & \end{array}$$

Note that folding (somewhat asymmetrically) the butterfly’s wings reproduces the pattern of (5.1). Thus, the moral is that the  $bc\beta\gamma$  realisation of  $N=2$  modules turns some of the mappings in (5.1) “inside out,” thus resulting in (1.1). The Felder resolution can be viewed similarly, with the “braid” of type (A.9) becoming an infinite line with the cohomology in the center. This has been given a precise meaning in [5]; an interesting question, therefore, is about the construction of the “intermediate” modules that interpolate between the 3, 5, 7, ...- and the butterfly resolutions.

As follows from the remarks made in the text, the butterfly resolution of the unitary  $\widehat{sl}(2)$  representations involves twisted (spectral-flow transformed) Wakimoto modules; with the  $\beta\gamma$  pictures being

different for different modules, this resolution can be viewed as pertaining to the three-boson realisation obtained by additionally bosonising the  $\beta\gamma$  fields in the Wakimoto representation.

From the LG perspective, relation (1.2) which characterises the unitary  $N=2$  representations, demonstrates a formal similarity with the unperturbed  $A_{p-1}$  LG equations of motion (suppressing the kinetic term)  $X^{p-1} = 0$ , Eq. (3.2); to continue with the parallel, moreover, recall that the chiral ring in the LG description is generated by  $1, X, \dots, X^{p-2}$ ; it turns out that the unitary  $N=2$  representations can be spanned by acting *solely with the modes*  $\mathcal{G}_n$ ,  $n \in \mathbb{Z}$ , subject to the constraints following from (1.2), with no other  $N=2$  generators involved [35]. Such a characterization of irreducible representations by a fermionic counterpart of the LG equations of motion would be extremely interesting to generalize to the case involving more than one ghost system of each sort.

*Acknowledgements.* We are grateful to I. Tipunin for very useful discussions. AMS is also grateful to V. Schomerus and K. Sfetsos for discussions on some related subjects, and to K. Sfetsos for pointing out the paper [20], in which several aspects of a later construction of [19] were anticipated. This work was supported in part by the RFBR Grant 98-01-01155.

#### APPENDIX A. $N=2$ VERMA MODULES

We first introduce the class of  $N=2$  Verma modules that we call *topological*<sup>8</sup> Verma modules following [19, 21]. For a fixed  $\theta \in \mathbb{Z}$ , we define the *twisted topological highest-weight vector*  $|h, t; \theta\rangle_{\text{top}}$  to satisfy the annihilation conditions (which are referred to as the twisted topological highest-weight conditions)

$$(A.1) \quad \mathcal{Q}_{-\theta+m}|h, t; \theta\rangle_{\text{top}} = \mathcal{G}_{\theta+m}|h, t; \theta\rangle_{\text{top}} = \mathcal{L}_{m+1}|h, t; \theta\rangle_{\text{top}} = \mathcal{H}_{m+1}|h, t; \theta\rangle_{\text{top}} = 0, \quad m \in \mathbb{N}_0,$$

with the following eigenvalues of the Cartan generators (where the second equation follows from the annihilation conditions):

$$(A.2) \quad (\mathcal{H}_0 + \frac{\varepsilon}{3}\theta)|h, t; \theta\rangle_{\text{top}} = h|h, t; \theta\rangle_{\text{top}},$$

$$(A.3) \quad (\mathcal{L}_0 + \theta\mathcal{H}_0 + \frac{\varepsilon}{6}(\theta^2 + \theta))|h, t; \theta\rangle_{\text{top}} = 0.$$

The parameter  $t$  fixes (the eigenvalue of) the central charge as  $c = 3(1 - \frac{2}{t})$ .

**Definition A.1.** The *twisted topological Verma module*  $\mathfrak{V}_{h,t;\theta}$  is the module freely generated from the topological highest-weight vector  $|h, t; \theta\rangle_{\text{top}}$  by  $\mathcal{Q}_{\leq -1-\theta}$ ,  $\mathcal{G}_{\leq -1+\theta}$ ,  $\mathcal{L}_{\leq -1}$ , and  $\mathcal{H}_{\leq -1}$ .

We write  $|h, t\rangle_{\text{top}} \equiv |h, t; 0\rangle_{\text{top}}$  in the ‘untwisted’ case of  $\theta = 0$  and also denote by  $\mathfrak{V}_{h,t} \equiv \mathfrak{V}_{h,t;0}$  the untwisted module.

Submodules in a topological Verma modules are twisted topological Verma modules (or a sum of two such modules). A singular vector exists in  $\mathfrak{V}_{h,t;\theta}$  if and only if  $h = \mathfrak{h}^+(r, s, t)$  or  $h = \mathfrak{h}^-(r, s, t)$ , where

$$(A.4) \quad \begin{aligned} \mathfrak{h}^+(r, s, t) &= \frac{1-r}{t} + s - 1, \\ \mathfrak{h}^-(r, s, t) &= \frac{1+r}{t} - s, \end{aligned} \quad r, s \in \mathbb{N}.$$

<sup>8</sup>chiral, in a different set of conventions, see, e.g., [36].



We denote these singular vectors  $|E(r, s, t)\rangle^{\pm, \theta}$ , respectively (omitting the twist  $\theta$  when it is equal to zero). The submodule of  $\mathfrak{V}_{h, t; \theta}$  generated from  $|E(r, s, t)\rangle^{\pm, \theta}$  is the twisted topological Verma module  $\mathfrak{V}_{h \pm r \frac{2}{t}, t; \theta \mp r}$ . When  $s = 1$ , the topological singular vectors take a particularly simple form,

$$(A.5) \quad |E(r, 1, t)\rangle^{+, \theta} = \mathcal{G}_{\theta-r} \dots \mathcal{G}_{\theta-1} |h^+(r, 1, t), t; \theta\rangle_{\text{top}},$$

$$(A.6) \quad |E(r, 1, t)\rangle^{-, \theta} = \mathcal{Q}_{-\theta-r} \dots \mathcal{Q}_{-\theta-1} |h^-(r, 1, t), t; \theta\rangle_{\text{top}},$$

while for  $s \geq 2$  singular vectors in topological Verma modules are given by the construction of [37, 21]. This involves the continued operators  $q(a, b)$  and  $g(a, b)$  that become the products  $\mathcal{Q}_a \mathcal{Q}_{a+1} \dots \mathcal{Q}_b$  and  $\mathcal{G}_a \mathcal{G}_{a+1} \dots \mathcal{G}_b$ , respectively, whenever  $b - a + 1 \in \mathbb{N}$ . In terms of these, the singular vectors read as

$$(A.7) \quad |E(r, s, t)\rangle^+ = g(-r, (s-1)t-1) \mathcal{E}^{-(s-1)t-r}(r, s-1, t) g((s-1)t-r, -1) |h^+(r, s, t), t\rangle_{\text{top}},$$

$$(A.8) \quad |E(r, s, t)\rangle^- = q(-r, (s-1)t-1) \mathcal{E}^{+, r-(s-1)t}(r, s-1, t) q((s-1)t-r, -1) |h^-(r, s, t), t\rangle_{\text{top}},$$

where  $\mathcal{E}^{\pm}$  are the corresponding singular vector *operators* and  $\mathcal{E}^{\pm, \theta}$  is their spectral flow transform by  $\theta$ . There exists a set of algebraic rules [21] that allow one to evaluate these expressions as monomials in the  $N=2$  generators  $\mathcal{Q}_n, \mathcal{G}_n, \mathcal{H}_n$ , and  $\mathcal{L}_n$ ,  $n \in \mathbb{Z}$ , once the singular vectors with  $s \mapsto s-1$  are evaluated in this form; with the  $s=1$  vectors given by (A.5) and (A.6), this gives a recursive procedure to evaluate all singular vectors in (twisted) topological Verma modules [37].

For  $t = p \in \mathbb{N} + 2$  and  $1 \leq r \leq p-1$ , the topological Verma module<sup>9</sup>  $\mathfrak{V}_{\frac{1-r}{p}, p; r-1}$  has the following embedding diagram [29, 16] consisting of twisted topological Verma modules, for which we indicate the  $h$  and  $\theta$  values as  $(h; \theta)$ :

$$(A.9) \quad \begin{array}{ccccccc} & & \left(\frac{r+1}{p}-2; p-1\right) & \left(\frac{1-r}{p}-2; p+r-1\right) & & \left(\frac{r+1}{p}-2m; mp-1\right) & \left(\frac{1-r}{p}-2m; mp+r-1\right) & & \dots \\ & \nearrow & \bullet & \xrightarrow{\quad} & \bullet & \nearrow & \bullet & \xrightarrow{\quad} & \bullet & \xrightarrow{\quad} & \dots \\ & \searrow & & \nwarrow & \nearrow & \searrow & & \nwarrow & \nearrow & & \dots \\ \left(\frac{1-r}{p}; r-1\right) & \bullet & & \bullet & & \bullet & & \bullet & & \bullet & \\ & \nwarrow & & \nwarrow & & \nwarrow & & \nwarrow & & \nwarrow & \\ & \bullet & \left(\frac{r+1}{p}; -1\right) & \left(\frac{1-r}{p}+2; r-1-p\right) & & \bullet & \left(\frac{r+1}{p}+2(m-1); (1-m)p-1\right) & \left(\frac{1-r}{p}+2m; r-1-mp\right) & & \bullet & \end{array}$$

The arrows are drawn in the direction of *submodules*. For Verma modules, such a digram represents the hierarchy of singular vectors and hence the “adjacency” of the irreducible subquotients. For Wakimoto-like modules, it is more natural to view similar diagrams as showing the adjacency of subquotients: every dot is an *irreducible* subquotient, and an arrow  $\bullet^A \rightarrow \bullet^B$  means that there exists a module in which  $B$  is a submodule and  $A$  is the quotient (this is often expressed by saying that  $A$  is glued to  $B$ ); thus, the arrows represent all the subquotients consisting of two irreducible ones.

A different class of Verma-like  $N=2$  modules are defined as follows [21].

<sup>9</sup>Where we start with the module twisted by  $r-1$  because we need this in Sec. 3; the overall twist can be applied to (A.9) straightforwardly, see [16].

**Definition A.2.** A twisted massive Verma module  $\mathfrak{U}_{h,\ell,t;\theta}$  is freely generated from a twisted *massive highest-weight vector*  $|h, \ell, t; \theta\rangle$  by the generators

$$(A.10) \quad \mathcal{L}_{-m}, m \in \mathbb{N}, \quad \mathcal{H}_{-m}, m \in \mathbb{N}, \quad \mathcal{Q}_{-\theta-m}, m \in \mathbb{N}_0, \quad \mathcal{G}_{\theta-m}, m \in \mathbb{N}.$$

The twisted massive highest-weight vector  $|h, \ell, t; \theta\rangle$  satisfies the following conditions:

$$(A.11) \quad \mathcal{Q}_{m+1-\theta} |h, \ell, t; \theta\rangle = \mathcal{G}_{m+\theta} |h, \ell, t; \theta\rangle = \mathcal{L}_{m+1} |h, \ell, t; \theta\rangle = \mathcal{H}_{m+1} |h, \ell, t; \theta\rangle = 0, \quad m \in \mathbb{N}_0,$$

$$(A.12) \quad (\mathcal{H}_0 + \frac{\varepsilon}{3}\theta) |h, \ell, t; \theta\rangle = h |h, \ell, t; \theta\rangle, \\ (\mathcal{L}_0 + \theta\mathcal{H}_0 + \frac{\varepsilon}{6}(\theta^2 + \theta)) |h, \ell, t; \theta\rangle = \ell |h, \ell, t; \theta\rangle.$$

We also write  $|h, \ell, t\rangle = |h, \ell, t; 0\rangle$  and  $\mathfrak{U}_{h,\ell,t} = \mathfrak{U}_{h,\ell,t;0}$ .

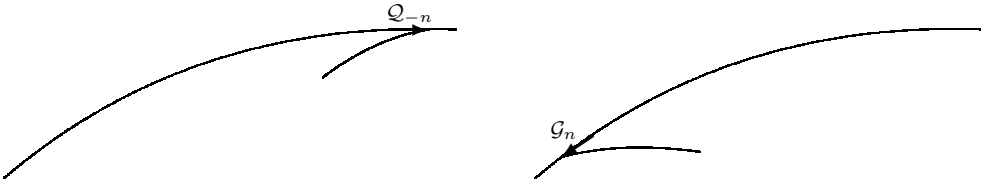
A *charged singular vector* occurs in  $\mathfrak{U}_{h,\ell,t;\theta}$  whenever [17]

$$(A.13) \quad \ell = \ell_{\text{ch}}(n, h, t) \equiv -n(h - \frac{n+1}{t}), \quad n \in \mathbb{Z},$$

and reads as [37, 21]

$$(A.14) \quad |E(n, h, t)\rangle_{\text{ch}}^\theta = \begin{cases} \mathcal{Q}_{-\theta-n} \dots \mathcal{Q}_{-\theta} |h, \ell_{\text{ch}}(n, h, t), t; \theta\rangle, & n \geq 0, \\ \mathcal{G}_{\theta+n} \dots \mathcal{G}_{\theta-1} |h, \ell_{\text{ch}}(n, h, t), t; \theta\rangle, & n \leq -1. \end{cases}$$

This state on the extremal diagram satisfies the *twisted* topological highest-weight conditions with the twist  $\theta + n$ , the submodule generated from  $|E(n, h, t)\rangle_{\text{ch}}^\theta$  being the twisted topological Verma module  $\mathfrak{V}_{h-\frac{2n}{t}-1, t; n+\theta}$  if  $n \geq 0$  and  $\mathfrak{V}_{h-\frac{2n}{t}, t; n+\theta}$  if  $n \leq -1$ . It is useful to represent the charged singular vectors, for  $n \geq 0$  and  $n \leq -1$  respectively, as follows:



(A.15)

Here, the arrows cannot be inverted by acting with the opposite mode of the other fermion from the  $N = 2$  algebra – which precisely means that the state obtained satisfies twisted *topological* highest-weight conditions and generates a *submodule*. In the body of the paper, we often deal with the charged singular vectors with  $n = 0$ , which exist in  $\mathfrak{U}_{h,0,p;\theta}$ , and those with  $n = -1$  in  $\mathfrak{U}_{h,h,p;\theta}$ . Note finally that whenever a charged singular vector generates a maximal submodule (i.e., is not contained in a submodule generated from another charged singular vector), the quotient of the massive Verma module over the corresponding submodule is a twisted topological Verma module.

## REFERENCES

- [1] B.L. Feigin and D.B. Fuchs, in: *Representations of Infinite-Dimensional Lie Groups and Algebras*, Gordon and Breach, 1989;  
*Representations of the Virasoro Algebra*, in: *Seminar on Supermanifolds*, D. Leites, ed.
- [2] I. Bernshtein, I. Gelfand, and S. Gelfand, *On the category of g-modules*, Funk. An. Prilozh. 10 (1976) 1.
- [3] G. Felder, *BRST Approach to Minimal Models*, Nucl. Phys. B317 (1989) 215, E: B324 (1989) 548.
- [4] D. Bernard and G. Felder, *Fock Representations and BRST Cohomology in SL(n) Current Algebra*, Commun. Math. Phys. 127 (1990) 145–168.

- [5] B.L. Feigin and E.V. Frenkel, *Representations of Affine Kac-Moody Algebras and Bosonization*, in: *Physics and Mathematics of Strings*, eds. L. Brink, D. Friedan, and A.M. Polyakov, World Sci.  
B.L. Feigin and E.V. Frenkel, *Affine Kac-Moody Algebras and Semi-Infinite Flag Manifolds*, Commun. Math. Phys. 128 (1990) 161–189.
- [6] P. Bouwknegt, J. McCarthy, and K. Pilch, *Quantum Group Structure in the Fock Space Resolutions of  $\widehat{sl}(n)$  Representation*, Commun. Math. Phys. 131 (1990) 125–155.
- [7] P. Fré, L. Girardello, A. Lerda, and P. Soriani, *Topological First-Order Systems with Landau-Ginzburg Interactions*, Nucl. Phys. B387 (1992) 333.
- [8] E. Witten, *On the Landau-Ginzburg Description of  $N=2$  Minimal Models*, Int. J. Mod. Phys. A9 (1994) 4783.
- [9] T. Kawai, Y. Yamada, and S.-K. Yang, *Elliptic Genera and  $N=2$  Superconformal Field Theory*, Nucl. Phys. B414 (1994) 191.
- [10] D. Nemeschansky and N.P. Warner, *The Refined Elliptic Genus and Coulomb Gas Formulations of  $N=2$  Superconformal Coset Models*, Nucl. Phys. B442 (1995) 623.
- [11] G. Mussardo, G. Sotkov, and M. Stanishkov,  *$N=2$  superconformal minimal models*, Int. J. Mod. Phys. A4 (1989) 1135.
- [12] N. Ohta and H. Suzuki,  *$N=2$  Superconformal Models and their Free Field Realizations*, Nucl. Phys. B332 (1990) 146.
- [13] K. Ito, *Quantum Hamiltonian Reduction and  $N=2$  Coset Models*, Phys. Lett. B259 (1991) 73; Nucl. Phys. B370 (1992) 123.
- [14] B. Gato-Rivera and A.M. Semikhatov,  *$d \leq 1 \cup d \geq 25$  and  $W$  Constraints from BRST-Invariance in the  $c \neq 3$  Topological Algebra*, Phys. Lett. B293 (1992) 72.
- [15] M. Bershadsky, W. Lerche, D. Nemeschansky, and N.P. Warner, *Extended  $N=2$  Superconformal Structure of Gravity and  $W$  Gravity Coupled to Matter*, Nucl. Phys. B401 (1993) 304.
- [16] B.L. Feigin, A.M. Semikhatov, V.A. Sirota, and I.Yu. Tipunin, *Resolutions and Characters of Irreducible Representations of the  $N=2$  Superconformal Algebra*, hep-th/9805179.
- [17] W. Boucher, D. Friedan, and A. Kent, *Determinant Formulae and Unitarity for the  $N=2$  Superconformal Algebras in Two-Dimensions or Exact Results on String Compactification*, Phys. Lett. B172 (1986) 316–322.
- [18] D.H. Friedan, E.J. Martinec, and S.H. Shenker, *Conformal Invariance, Supersymmetry and String Theory*, Nucl. Phys. B271 (1986) 93.
- [19] B.L. Feigin, A.M. Semikhatov, and I.Yu. Tipunin, *Equivalence between Chain Categories of Representations of Affine  $sl(2)$  and  $N=2$  Superconformal Algebras*, hep-th/9701043, J. Math. Phys. 39 (1998) 3865–3905.
- [20] L.J. Dixon, M.E. Peskin, and J. Lykken,  *$N=2$  Superconformal Symmetry and  $so(2,1)$  Current Algebra*, Nucl. Phys. B325 (1989) 329.
- [21] A.M. Semikhatov and I.Yu. Tipunin, *The Structure of Verma Modules over the  $N=2$  Superconformal Algebra*, Commun. Math. Phys. 195 (1998) 129–173.
- [22] A.S. Losev (Losev), *Descendants Constructed from Matter Field and K. Saito Higher Residue Pairing in Landau-Ginzburg Theories Coupled to Topological Gravity*, hep-th/9211090.
- [23] T. Eguchi, H. Kanno, Y. Yamada and S.-K. Yang, *Topological Strings, Flat Coordinates and Gravitational Descendants*, Phys. Lett. B305 (1993) 235.
- [24] W. Lerche and N.P. Warner, *On the Algebraic Structure of Gravitational Descendants in  $CP(n-1)$  Coset Models*, Phys. Lett. B343 (1995) 87.
- [25] A. Schwimmer and N. Seiberg, *Comments on the  $N=2$ ,  $N=3$ ,  $N=4$  Superconformal Algebras in Two-Dimensions*, Phys. Lett. B184 (1987) 191.
- [26] M. Wakimoto, *Fock Representations of the Affine Lie Algebra  $A_1^{(1)}$* , Commun. Math. Phys. 104 (1986) 605–609.
- [27] B.L. Feigin and E.V. Frenkel, *A Family of Representations of Affine Lie Algebras*, Usp. Mat. Nauk 43 no. 5 (1988) 227–228.
- [28] A. Gerasimov, A. Marshakov, A. Morozov, M. Olshanetsky, and S. Shatashvili, *Wess-Zumino-Witten Models as a Theory of Free Fields*, Int. J. Mod. Phys. A5 (1990) 2495–2589.
- [29] A.M. Semikhatov and V.A. Sirota, *Embedding Diagrams of  $N=2$  and Relaxed- $\widehat{sl}(2)$  Verma Modules*, hep-th/9712102.
- [30] E. Verlinde and H. Verlinde, *A Solution of Two-Dimensional Topological Quantum Gravity*, Nucl. Phys. B348 (1991) 457.  
R. Dijkgraaf, E. Verlinde, and H. Verlinde, *Notes on Topological String Theory and 2d Quantum Gravity*, PUPT-1217, IASSNS-HEP-90/80.
- [31] K. Landsteiner, W. Lerche and A. Sevrin, *Topological Strings from WZW Models*, Phys. Lett. B352 (1995) 286.
- [32] W. Lerche, *Generalized Drinfeld-Sokolov Hierarchies, Quantum Rings, and  $W$ -Gravity*, Nucl. Phys. B434 (1995) 445–474; *Chiral Rings and Integrable Systems for Models of Topological Gravity*, hep-th/9401121.
- [33] R. Dijkgraaf, E. Verlinde, and H. Verlinde, *Topological Strings in  $d < 1$* , Nucl. Phys. B352 (1991) 59.
- [34] A.M. Semikhatov and I.Yu. Tipunin, unpublished.

- [35] B.L. Feigin, A.M. Semikhatov, and I.Yu. Tipunin, *A Semi-Infinite Realization of Unitary Representations of the  $N=2$  Superconformal Algebra*, to appear.
- [36] W. Lerche, C. Vafa, and N.P. Warner, *Chiral Rings In  $N=2$  Superconformal Theories*, Nucl. Phys. B324 (1989) 427.
- [37] A.M. Semikhatov and I.Yu. Tipunin, *All Singular Vectors of the  $N = 2$  Superconformal Algebra via the Algebraic Continuation Approach*, hep-th/9604176.

LANDAU INSTITUTE FOR THEORETICAL PHYSICS, RUSSIAN ACADEMY OF SCIENCES

TAMM THEORY DIVISION, LEBEDEV PHYSICS INSTITUTE, RUSSIAN ACADEMY OF SCIENCES